Russian Chemical Reviews **72** (6) 471 – 488 (2003) © 2003 Russian Academy of Sciences and Turpion Ltd

DOI 10.1070/RC2003v072n06ABEH000808

The photorefractive effect in polymeric systems

A V Vannikov, A D Grishina

Contents

I.	Introduction	471
II.	Nature of the photorefractive effect in polymers	472
III.	The figure of merit of nonlinear optical chromophores	476
IV.	Interrelation between the photorefractive effect and the photoelectric and electron transport properties	479
V.	The gain coefficient and diffraction efficiency in photorefractive polymeric systems	483
VI.	Practical applications of polymeric photorefractive materials	485

Abstract. The review concerns the photorefractive effect in polymeric systems, which involves the creation, upon a primary photochemical reaction, of a phase grating shifted in space relative to the fringe pattern. The interaction of interfering laser beams accompanied by energy transfer from one beam to the other as well as salient features of the refractive index modulation in polymeric systems with low and high glass transition temperatures are considered. Particular attention is given to the photorefractive polymers with high glass transition temperatures containing nanocrystalline J-aggregates of cyanine dyes, which are characterised by high third-order nonlinear electric susceptibilities and induce modulation of the refractive index due to the Kerr electro-optic effect. The prospects for application of polymeric photorefractive materials are outlined. The bibliography includes 113 references.

I. Introduction

The photorefractive (PR) effect is induced by two interfering laser beams (a pump beam and a signal beam) and consists in reversible creation of a phase grating, which is shifted in space relative to the bright fringes. As a consequence, the pump beam reflected from the grating travels parallel to and is in phase with the signal beam. After passing the PR system the intensity of the signal beam is amplified at the attenuation of the reflected pump beam. The reflected signal beam is out of phase with the pump beam; therefore, the intensity of the latter decreases.

The photorefractive effect arises in polymeric media possessing specific properties. First, they must exhibit photoelectric sensitivity and provide the possibility of photogeneration of charge carriers of both signs in bright regions of the interference pattern as a result of a primary photochemical reaction and subsequent charge separation and transport. In most polymeric systems electrons are trapped by deep traps near the generation sites in bright regions of the interference pattern, while holes drift in the applied electric field E_0 towards the dark regions of the interference pattern until trapping. As a result, a periodic space-charge field E_{sc} is induced, which is shifted in space relative to the fringe pattern. Second, polymeric systems must contain some compounds (chromophores) possessing second- or third-order nonlinear optical properties and/or anisotropy of the linear polarisability (*e.g.*, dipole molecules of organic compounds with electron-donor and electron-acceptor substituents). The orientational or electronic polarisation of chromophores in the periodic field E_{sc} is responsible for periodic modulation of the refractive index, *i.e.*, creation of a phase grating whose maxima coincide with those of the periodic field E_{sc} and, hence, are shifted in space relative to the interference fringes.

Photorefraction was first observed in inorganic crystals $LiNbO_3$ and $LiTaO_3$ in 1966.[1] In 1990, the phenomenon was reported for organic crystals[2] and in 1991 for polymeric composites.[3,4] Recently, interest in photorefraction in the polymeric materials has increased due to the possibility of using them as highly efficient active optical elements for data transmission and controlling coherent radiation in various electro-optical and optical communication devices. Pioneering attempts to employ photorefractive polymeric materials for writing holograms of moving objects were due to the high writing and erasing speed of such materials. Polymeric systems are also of considerable interest because their spectral properties can be smoothly varied by changing the structure of polymers and polymeric composites. There is a great potential of doping such systems; in addition, they are cheap, readily processable and allow fabrication of parts of any shape and size which are compatible with moderm microelectronic and optoelectronic devices, *etc*.

Recently, various types of photorefractive polymeric materials have been designed. These are polymers in which functional groups (namely, sensitisers responsible for the photoelectric sensitivity, charge transport sites and nonlinear optical chromophores) are constituents of the main polymer chain or bound to it as side substituents; 'guest – host' composites (functionally doped polymers possessing the charge transport properties); and polymer layers modified in one or another manner (*e.g.*, photochemically). Often, bifunctional polymeric systems are prepared, in which the same chain fragment or dopant simultaneously exhibits the properties of sensitiser and a chromophore or a charge transport site.

In preparing the manuscript the authors of this review focussed on the most interesting, from their viewpoint, results rather than comprehensive consideration of numerous available studies on the title problem.

A V Vannikov, A D Grishina A N Frumkin Institute of Electrochemistry, Russian Academy of Sciences, Leninsky prosp. 31, 119071 Moscow, Russian Federation. Fax (7-095) 952 08 46. Tel. 952 31 22.
E-mail: van@elchem.ac.ru

Received 23 December 2002
Uspekhi Khimii **72** (6) 531 – 549 (2003); translated by A M Raevsky

II. Nature of the photorefractive effect in polymers

The most informative method for studying the PR effect is the two-beam method (Fig. 1). It involves splitting of a laser beam into two beams, which reflect from mirrors and then intersect inside a polymer layer. Each beam is characterised by the

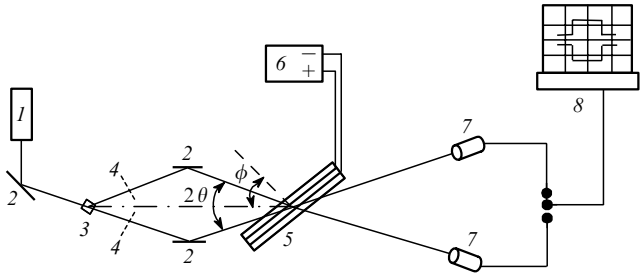


Figure 1. A scheme for measuring the PR effect.
Laser (*1*), reflecting mirrors (*2*), beam splitter (*3*), shutters for beams **1** and **2** (*4*), sample (*5*), constant voltage source (*6*), photodiodes (*7*), computer (*8*); 2θ is the angle between beam **1** and beam **2**; ϕ is the angle between the z axis (bisectrix of the 2θ angle) and the normal to the surface of the sample.

amplitude, $E_{1,2}(\omega)$, or intensity, $I_{1,2} \sim E_{1,2}^2$, of the electric component of the electromagnetic field. Interference causes a periodic distribution of the light intensity (I) in space

$$\frac{I}{I_1 + I_2} = 1 + 2\frac{(I_1 I_2)^{0.5}}{I_1 + I_2}\cos\left(\frac{2\pi x}{\Lambda}\right). \tag{1}$$

Here x is the coordinate along the x axis directed normal to the bisectrix of the 2θ angle between the beams (Fig. 2 *a*); Λ is the spatial period (Fig. 2 *b*), *i.e.*, the distance between the bright fringes [or constructive interference fringes, where $\cos(2\pi x/\Lambda) = 1$)] along the x axis

$$\Lambda = \frac{\lambda}{\sin\theta},$$

$\lambda = \lambda_0/n$ is the optical wavelength in the polymer; λ_0 is the free-space wavelength; and n is the refractive index of the polymer.

A feature of systems exhibiting photoelectric sensitivity is photogeneration of charge carriers in the constructive interference regions. The number of charge carriers generated is proportional to the light intensity modulation, m (Ref. 5)

$$m = 2\frac{(I_1 I_2)^{0.5}}{I_1 + I_2}.$$

The necessary condition for the PR effect is considerable difference between the mobilities of photochemically generated electrons and holes. For most polymeric media the mobility of electrons is much lower than that of holes. Electrons are trapped in the regions of bright fringes, while holes drift in the constant electric field E_0 towards the dark regions [or the destructive interference regions, where $\cos(2\pi x/\Lambda) = -1$]. This leads to separation of charge carriers in space and to the appearance of a periodic space-charge electric field E_{sc}, which is directed perpendicular to the bisectrix of the angle between the incident beams and shifted in phase by ψ relative to the fringe pattern (see Fig. 2 *b*)

$$E_{sc} = E_{sc}^0 \cos\left(\frac{2\pi x}{\Lambda} - \psi\right). \tag{2}$$

The E_{sc}^0 field is proportional to the concentration of charge carriers generated in bright regions or, ultimately, to the light intensity modulation

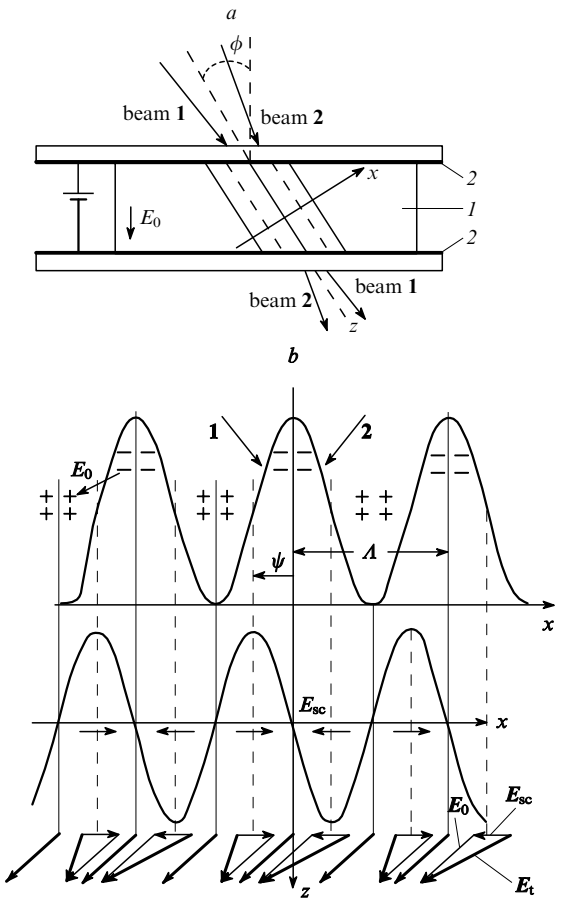


Figure 2. Measuring cell geometry (*a*) and a scheme illustrating the nature of the PR effect in polymeric systems (*b*);
(*a*) polymer layer (*1*), electrodes made of transparent conducting In_2O_3 : Sn film supported by glass slides; regions of constructive and destructive interference in the polymer layer are denoted by the solid and dashed lines, respectively; (*b*) the fringe pattern and photogeneration of charge carriers, the $\boldsymbol{E}_{sc}$ field distribution along the x axis and the distribution of the total field, $\boldsymbol{E}_t = \boldsymbol{E}_{sc} + \boldsymbol{E}_0$, in the polymer layer (thick arrows); the '$-$' signs in the interference-maximum regions denote trapped electrons; the '$+$' signs denote holes migrated to the interference-minimum regions in the $\boldsymbol{E}_0$ field; ψ is the shift in space of the phase of the $\boldsymbol{E}_{sc}$ field relative to the fringe pattern; the $\boldsymbol{E}_{sc}$ vector is parallel to the x axis and the $\boldsymbol{E}_0$ vector is directed from the anode to the cathode.

$$E_{sc}^0 \sim 2\frac{(I_1 I_2)^{0.5}}{I_1 + I_2}. \tag{2a}$$

If positive charges are located at the midpoints of dark regions, the E_{sc} field has maxima at the midpoints between bright and dark fringes, *i.e.*, these maxima are shifted by $x = \Lambda/4$ or by a phase of $\psi \approx \pi/2$ in space relative to the bright fringes. However, the phase shift is usually less than $\pi/2$.

If a composite contains chromophores possessing nonlinear optical properties or anisotropy of the linear polarisability, the E_{sc} field induces a periodic distribution of the refractive index. Indeed, the refractive index is related to the linear electric susceptibility of a unit volume of a polymeric composite [$\chi^{(1)}$] as follows:

$$n^2 = 1 + 4\pi\chi^{(1)}. \tag{3}$$

The electric susceptibility,

$$\chi^{(1)} = \frac{P(\omega)}{E(\omega)},$$

characterises the linear polarisation, $P(\omega)$, of a unit volume of a substance, induced by the electric component, $E(\omega)$, of the electromagnetic field vector of the light wave. As will be shown below, $\chi^{(1)}$ becomes a variable quantity in a constant electric field.

A feature of non-centrosymmetric chromophores (dipole molecules containing electron-donor and electron-acceptor groups) is that displacement of the electron density from the donor group to the acceptor group induced by the $E(\omega)$ field is larger than in the opposite direction. If the dipole chromophores in the bulk of a substance are aligned in some way during the preparation of a polymer layer, stimulated radiation of an ensemble of such chromophores is anharmonic and can be represented by a set of Fourier components with frequencies ω, 2ω, *etc.*[6–9] Otherwise, the dipole chromophores are disordered. The second-order susceptibility is given by the formula

$$\chi^{(2)} = Nf(\omega)\beta\langle\cos^3\varphi\rangle,$$

where N is the number of chromophores per unit volume; $f(\omega) = (n^2 + 2)/3$ is the correlation factor relating the external electric field of electromagnetic wave to the field in the medium; β is the second-order molecular polarisability; and $\langle\cos^3\varphi\rangle$ is a parameter characterising the averaged value of the angle of rotation of the dipole moments of chromophores about a specified axis.

For centrosymmetric media (random distribution of the dipole moments of N chromophores), $\langle\cos^3\varphi\rangle = 0$ and the second-order nonlinear susceptibility vanishes. If rotational diffusion of chromophores is possible in a medium, they are aligned in the electric field E_0. Rotational diffusion of chromophores in polymeric systems is efficient only at temperatures above the glass transition temperature (T_g); therefore, experiments with high-T_g polymers require preliminary alignment in the polarising electric field E_p at $T_p > T_g$. Such an alignment is retained on subsequent cooling ('freezing') of the system in the field E_p down to temperatures below T_g. According to the Langevin formula,

$$\langle\cos^3\varphi\rangle = \frac{f(0)E_p\mu_g}{5kT},$$

where $f(0)$ is the correlation factor relating the external applied field E_p to the field in the polymer layer,

$$f(0) = \varepsilon\frac{n^2+2}{2\varepsilon+n^2}$$

(ε is the dielectric constant); and μ_g is the ground-state dipole moment of the chromophore. The formula for the second-order nonlinear volume susceptibility of high-T_g polymers has the form

$$\chi^{(2)} = \frac{Nf(\omega)f(0)\beta E_p\mu_g}{5kT}. \tag{4}$$

At room temperature, chromophores in plasticised polymers (T_g is below the temperature of the experiment, ~ 20 °C) are in the mobile state and their alignment makes no sense, since they again become randomly distributed after switching the E_p field off. In such polymers the second-order susceptibility arises only in a constant field. Taking into account the fact that the $\chi^{(2)}$ value is determined by the total field

$$\boldsymbol{E}_t = \boldsymbol{E}_{sc} + \boldsymbol{E}_0,$$

we get

$$\chi^{(2)} = \frac{Nf(\omega)f(0)\beta E_t\mu_g}{5kT}. \tag{4a}$$

The distributions of the $\boldsymbol{E}_t$ field and the $\boldsymbol{E}_{sc}$ and $\boldsymbol{E}_0$ components along the x axis are shown in Fig. 2*b*.

The E_t field is involved in the electronic polarisation of a molecule along with the light wave field, $E(\omega)$; therefore, the expression for the volume polarisation, $P(E)$, can be written as follows:

$$\begin{aligned} P(E) = {} & [\chi_E^{(1)}(-\omega,\omega) + \chi^{(2)}(-\omega,\omega,0)f(0)E_t + \\ & + \chi^{(3)}(-\omega,\omega,0,0)f^2(0)E_t^2]f(\omega)f(-\omega)E(\omega) + \\ & + [\chi^{(2)}(-2\omega,\omega,\omega) + \\ & + \chi^{(3)}(-2\omega,\omega,\omega,0)f(0)E_t]f^2(\omega)f(-2\omega)E^2(\omega) + \\ & + \chi^{(3)}(-3\omega,\omega,\omega,\omega)f^3(\omega)f(-3\omega)E^3(\omega). \end{aligned} \tag{5}$$

Here $\chi_E^{(1)}$ is the linear volume susceptibility in the constant field; $\chi^{(2)}$ and $\chi^{(3)}$ are the second- and third-order nonlinear volume susceptibilities, respectively; $(-\omega)$, (-2ω) and (-3ω) are the frequencies of the first, second and third harmonics of stimulated radiation of the ensemble of oscillating dipoles when the laser operates at the fundamental frequency ω.

Taking into account formula (5), the linear electric susceptibility in the presence of a constant field E_0 and the E_{sc} field is

$$\chi^{(1)} = \chi_E^{(1)} + f(0)E_t\left[\chi^{(2)} + \chi^{(3)}f(0)E_t\right],$$

while relationship (3) takes the form

$$n_E^2 = 1 + 4\pi\left[\chi_E^{(1)} + E_t(\chi^{(2)} + \chi^{(3)}E_t)\right]. \tag{5a}$$

[hereafter the $f(0)$ factor is omitted].

The refractive index modulation (grating amplitude) is determined by the difference between expression (5a) in the presence of the E_t field and expression (3) in the presence of the E_0 field, when $\chi^{(1)} = \chi_0^{(1)}$,

$$\Delta n = \frac{n_E^2 - n^2}{n_E + n}.$$

Assuming $n_E + n = 2n$, we get

$$\Delta n = \frac{2\pi}{n}\left[E_{sc}(\chi^{(2)} + \chi^{(3)}E_t) + \chi_E^{(1)} - \chi_0^{(1)}\right]. \tag{6}$$

This relation demonstrates that generally three effects contribute to the creation of the phase grating. The first and second effects (the first two terms) are the refractive index modulations due to the Pockels electro-optic effect (PEO) and the quadratic Kerr electro-optic effect (KEO)

$$\Delta n_1 = \Delta n_{PEO} + \Delta n_{KEO}, \tag{7}$$

where

$$\Delta n_{PEO} = \frac{2\pi}{n}\chi^{(2)}E_{sc},$$

$$\Delta n_{KEO} = \frac{2\pi}{n}\chi^{(3)}E_{sc}E_t.$$

According to the known formula [6] of the electro-optic effect,

$$\Delta n_1 = \frac{n^3}{2}E_t(r + sE_t)$$

the linear Pockels electro-optical coefficient r is proportional to the susceptibility, $\chi^{(2)}$, while the quadratic Kerr electro-optical coefficient s is related to the $\chi^{(3)}$ susceptibility.

The other terms in formula (6)

$$\Delta n_2 = \frac{2\pi\left(\chi_E^{(1)} - \chi_0^{(1)}\right)}{n}$$

are the refractive index modulations due to alignment of dipole chromophores along the E_t field. This effect is characteristic of plasticised layers only and is not observed in high-T_g polymeric

systems. Due to orientational birefringence, OB, the refractive index modulation is described as follows:[10–13]

$$\Delta n_{\mathrm{OB}} = \frac{2\pi}{n}\left(\chi_E^{(1)} - \chi_0^{(1)}\right) = \frac{2\pi}{n} N\Delta\alpha\left(\langle\cos^2\varphi\rangle - \frac{1}{3}\right) \approx \quad (8)$$

$$\approx \frac{2\pi}{n}\,\frac{4Nf^2(0)f(\omega)}{45}\Delta\alpha(-\omega,\omega)\left(\frac{\mu_g E_t}{kT}\right)^2,$$

where $\Delta\alpha$ is the anisotropy of the linear polarisability

$$\Delta\alpha = \alpha_{||} - \alpha_{\perp},$$

and $\alpha_{||}$ and $\alpha_{\perp}$ are the molecular polarisabilities along and normal to the principal axis of a dipole chromophore, respectively.

For an isotropic medium, $\langle\cos^2\varphi\rangle = 1/3$; therefore, the volume anisotropy of the linear polarisability vanishes [see formula (8)]. A two-level model of polarisation [14] describes the anisotropy of polarisability, $\Delta\alpha(-\omega,\omega)$, by the relationship

$$\Delta\alpha(-\omega,\omega) = \Delta\alpha(0)\,\frac{E_{ge}^2}{E_{ge}^2 - (h\omega)^2},$$

where $\Delta\alpha(0) = 2\mu_{ge}^2/E_{ge}$ and μ_{ge} and E_{ge} are the dipole moment and energy of transition from the ground state to the excited state, respectively. Since the OB is due to rotational diffusion of a dipole chromophore during the formation of the E_t field, the parameter Δn_{OB} significantly contributes to the refractive index modulation of those liquid crystals or plasticised polymers whose glass transition temperatures are low (close to room temperature).[10,12,15] Creation of orientational grating was established in liquid-crystalline media [16–18] and polymeric composites.[10] Liquid crystals are characterised by the largest orientational refractive index modulation due to strong dielectric anisotropy.[11,13,17–19]

The photorefractive effect in nonlinear optical materials is determined by the spatial modulation of the refractive index (see above).[4]

Creation of a grating in polymer layers of thickness d meeting the following criterion

$$Q = \frac{\pi d\lambda}{\Lambda^2 n} > 1,$$

(more preferable, $Q > 5$, see Ref. 12) is accompanied by self-diffraction of beams due to the Bragg scattering (reflection). Beam **1** is reflected towards beam **2**, while beam **2** is reflected towards beam **1**. For the measuring cell geometry shown in Fig. 2 *a* the reflected beam **1** is in phase with beam **2**. Beam mixing causes an increase in the intensity of the output beam **2** and a decrease in the intensity of the output beam **1** because the reflected beam **2** and beam **1** are out of phase.

The main formulae suitable for estimation of the PR parameters (*e.g.*, the two-beam coupling gain Γ, phase shift of the grating, *etc.*), were obtained by solving the Kogelnik coupled-wave equations,[20] according to which a change in the amplitude (or $I^{0.5}$) of each beam along the z axis is proportional to the amplitude of the other beam and the refractive index modulation, Δn (see Refs 5, 20–23)

$$\frac{\partial(I_1)^{0.5}}{\partial z} = -\left(\frac{\pi\Delta n}{\lambda}\right)(I_2)^{0.5}, \quad (9)$$

$$\frac{\partial(I_2)^{0.5}}{\partial z} = -\left(\frac{\pi\Delta n}{\lambda}\right)(I_1)^{0.5}. \quad (10)$$

The most important relationships were obtained for the PR effect in inorganic crystals assuming that $\Delta n \sim E_{sc}$.[5,21,22] Taking into account formulae (2) and (2a), in this case one can write [5,22–28]

$$\Delta n = \Delta n_{\max}\,\frac{2(I_1 I_2)^{0.5}}{I_1 + I_2}\cos\left(\frac{2\pi x}{\Lambda} - \psi\right).$$

Beam **2** reflected from the PR grating in the $\Delta n_{\max}$ region travels now in the same direction as does beam **1** (the angle of incidence equals the angle of reflection), *i.e.*, towards positive x values (see Fig. 2 *b*). Therefore Eqn (9) can be rewritten as follows:[22]

$$\frac{\partial(I_1)^{0.5}}{\partial z} = -2\left(\frac{\pi\Delta n_{\max}}{\lambda}\right)\frac{(I_2)^{0.5}(I_1 I_2)0.5}{I_1 + I_2}\cos\left(\frac{2\pi x}{\Lambda} - \psi\right). \quad (9a)$$

Simultaneously the reflected beam **1** propagates in the same direction as does beam **2** (towards negative x values). Then, formula (10) takes the form [22]

$$\frac{\partial(I_2)^{0.5}}{\partial z} = -2\left(\frac{\pi\Delta n_{\max}}{\lambda}\right)\frac{(I_1)^{0.5}(I_1 I_2)^{0.5}}{I_1 + I_2}\cos\left(-\frac{2\pi x}{\Lambda} - \psi\right). \quad (10a)$$

In accord with the energy conservation law

$$I_1(0) + I_2(0) = \frac{I_1(z) + I_2(z)}{\exp(-\alpha z)} = \frac{I_1(L) + I_2(L)}{\exp(-\alpha L)}.$$

Here $I_1(z) \equiv I_1$ and $I_2(z) \equiv I_2$; $\alpha = 2.3A/d$ is the absorption coefficient (A is the optical absorption at the laser wavelength and d is the layer thickness); $I_1(0)$, $I_2(0)$ and $I_1(L)$, $I_2(L)$ are the intensities of the input and output beams, respectively; $L = d/\cos(\phi - \theta)$ is the optical path of beam **2** (see Fig. 2 *a*). Let us denote $I_1(0) + I_2(0) = I_0$. To simplify the solutions, suppose that $\alpha = 0$; then, after replacing I_2 by $(I_0 - I_1)$ in Eqn (9a) we get

$$\frac{\partial(I_1)^{0.5}}{I_1^{0.5}(I_0 - I_1)} = -2\,\frac{\pi\Delta n_{\max}}{\lambda I_0}\,\partial z \times \quad (11)$$

$$\times\left[\cos\left(\frac{2\pi x}{\Lambda}\right)\cos\psi + \sin\left(\frac{2\pi x}{\Lambda}\right)\sin\psi\right].$$

Analogous substitution into Eqn (10a) for beam **2** ($I_1 = I_0 - I_2$) gives

$$\frac{\partial(I_2)^{0.5}}{I_2^{0.5}(I_0 - I_2)} = -2\,\frac{\pi\Delta n_{\max}}{\lambda I_0}\,\partial z \times \quad (11a)$$

$$\times\left[\cos\left(\frac{2\pi x}{\Lambda}\right)\cos\psi - \sin\left(\frac{2\pi x}{\Lambda}\right)\sin\psi\right].$$

Relationships (11) and (11a) thus obtained are unsymmetric, namely, the second terms on the right-hand sides of the equations (they are responsible for energy transfer from beam **1** to beam **2**) have opposite signs (negative sign for beam **1** and positive sign for beam **2**).[22] The energy transfer coefficient, or the two-beam coupling gain, can be found by subtracting relatonship (11) from Eqn (11a). After integration of this difference at a particular x value (*e.g.*, at $x = \Lambda/4$), one gets [5]

$$\ln\frac{I_2(L)\beta}{I_1(L)} = \Gamma L, \quad (12)$$

where $\beta = I_1(0)/I_2(0)$,

$$\Gamma = \frac{4\pi\Delta n_{\max}\sin\psi}{\lambda}. \quad (12a)$$

From Eqn (12) it follows that

$$I_1(L) = I_2(L)\beta e^{-\Gamma L}.$$

Hence

$$I_1(L) + I_2(L) = I_2(L)\beta e^{-\Gamma L} + I_2(L) = I_2(L)(1 + \beta e^{-\Gamma L}).$$

At the same time, in accord with the energy conservation law one has

$$I_2(L) + I_1(L) = [I_2(0) + I_1(0)]e^{-\alpha L} = I_2(0)(1 + \beta)e^{-\alpha L},$$

i.e.,

$$I_2(L)(1 + \beta e^{-\Gamma L}) = I_2(0)(1 + \beta)e^{-\alpha L}$$

or

$$\frac{I_2(L)}{I_2(0)} = \frac{(1+\beta)e^{-\alpha L}}{1+\beta e^{-\Gamma L}}. \quad (13)$$

Formula (13) serves for estimation of the amplification of the information beam **2** at different β, Γ and α. Experimental estimation of the gain involves measurements of the beam coupling ratio (γ_0)

$$\gamma_0 = \frac{I_2(L)_t}{I_2(L)_{t=0}}. \quad (14)$$

Here the $I_2(L)_t$ value (beam **1** is on) is determined by relationship (13). If beam **1** is switched off [$I_1(0) = 0$ and $\beta = 0$], one gets $I_2(L)_{t=0} = I_2(0)\exp(-\alpha L)$. Thus, the formula (14) for the beam coupling ratio takes the form

$$\gamma_0 = \frac{1+\beta}{1+\beta\exp(-\Gamma L)}.$$

From here the two-beam coupling gain, Γ, can be calculated using the formula

$$\Gamma L = \ln\frac{\gamma_0\beta}{1+\beta-\gamma_0}. \quad (15)$$

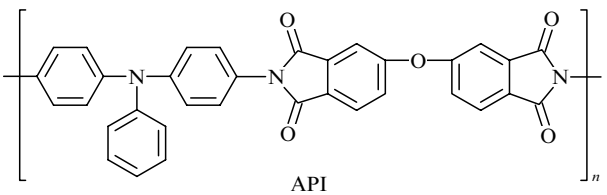
The γ_0 value is estimated from that portion of the kinetic curve, which corresponds to saturation of the beam coupling ratio.

Thus, a shift of the phase grating in space relative to the constructive interference fringes provides amplification of beam **2** due to attenuation of beam **1**. As the polarity of the applied voltage (*i.e.*, the E_0 sign) changes (see Fig. 2 *a*), photogenerated mobile holes migrate in the opposite direction relative to that shown in Fig. 2 *b* and the grating is shifted by a phase of ψ towards positive x values

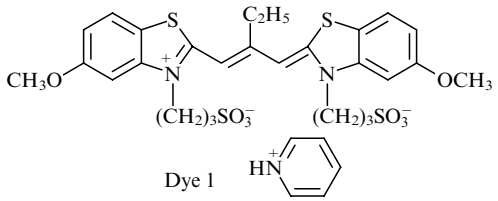
$$\Delta n = \Delta n_{\max}\left[\frac{2(I_1I_2)^{0.5}}{I_1+I_2}\right]\cos\left(\frac{2\pi x}{\Lambda}+\psi\right).$$

In this case beam **1** is amplified, while beam **2** becomes the pump beam. The beam directed from the fringe to the grating is amplified (see Fig. 2 *a*).

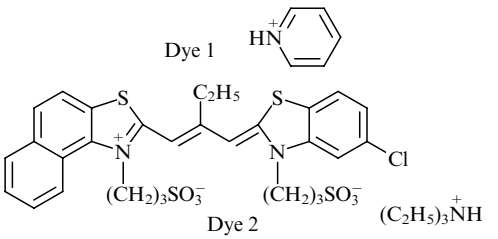
As will be shown below, polymeric composites containing nanocrystalline J-aggregates of cyanine dyes (dipole molecules aligned to form the 'head-to-tail' chains) occupy a special position among photorefractive polymeric materials. Figure 3 presents the kinetic curves for two-beam coupling measured for aromatic polyimide (API) containing J-aggregates of thiacarbocyanine dyes (Dye 1 and Dye 2, respectively).[29, 30]



API



Dye 1



Dye 2

Measurements were carried out at $\beta = I_1(0)/I_2(0) = 1$. The experimental design was as follows. The first experiment involved measurements of the beam **1** intensity. First, beam **1** was switched on. At $t = 0$, the E_0 field was applied to the sample and then beam **2** was switched on (upward arrow). This resulted in a decrease in the beam **1** intensity (curve *1*). The intensities of the output beam **1** with beam **2** off and on are denoted as $I_1(L)_{t=0}$ and $I_1(L)_t$, respectively. After the curve reached saturation, beam **2** was switched off (downward arrow) and, as can be seen, the initial beam **1** intensity, $I_1(L)_{t=0}$, was restored. Then the same operations were repeated for beam **2**. First, beam **2** was switched on and then the E_0 field was applied, the $I_2(L)_{t=0}$ value was measured and beam **1** was switched on. This led to an increase

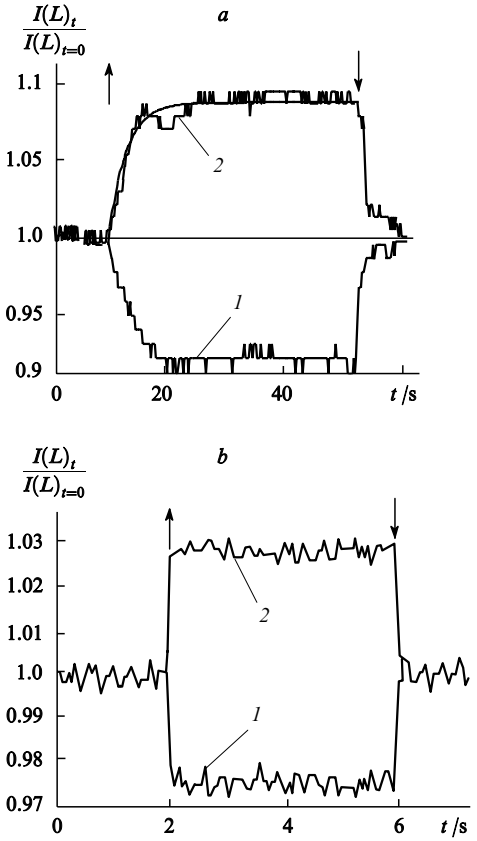


Figure 3. Kinetic curves for two-beam coupling in a polymeric composite [API containing J-aggregates of Dye 1 (*a*) and Dye 2 (*b*)].[29, 30] Experimental conditions: an Ar–Kr laser (647 nm), $I_1(0) = I_2(0) = 0.03$ W cm^{-2}, $E_0 = 16$ V μm^{-1}. Changes in the beam **1** intensity upon switching beam **2** on (upward arrow) and off (downward arrow) (*1*) and changes in the beam **2** intensity upon switching beam **1** on (upward arrow) and off (downward arrow) (*2*).

in the beam **2** intensity, $I_2(L)_t$ (curve *2*). After switching beam **1** off the intensity of beam **2** took its initial value $I_2(L)_{t=0}$. The $I_2(L)_t/I_2(L)_{t=0}$ ratio is the beam coupling ratio, γ_0, at saturation [see Eqn (14)]. As the refractive index modulation is created, the intensity of beam **1** (pump beam) decreases, while the intensity of beam **2** (signal beam) increases to nearly the same extent (see Fig. 3). This unambiguously points to writing of a phase grating, which is shifted in space relative to the fringe pattern (see Fig. 2 *b*).

The most important characteristics of the PR effect are the two-beam coupling gain, Γ (more rigorously, the net internal gain, $\Gamma-\alpha$), Δn_{max}, the diffraction efficiency, η, and the response time, τ, of the polymeric composite to the two-beam coupling. The last-mentioned parameter is 3 s for the API/Dye 1 composite (see Fig. 3 *a*) and less than 20 ms (the temporal resolution of the experimental setup) for the API/Dye 2 composite (see Fig. 3 *b*).

The diffraction efficiency (in %) is defined by the following relation:[21]

$$\eta = 100\sin^2\left(\frac{\pi\Delta n_{max}d}{\lambda\cos\theta}\right). \quad (16)$$

Experiments on determination of the diffraction efficiency involve the use of two writing beams to create a grating which is read out with the third beam (readout beam of intensity I_3) propagating parallel to beam **1** (or **2**). Beam **3** diffracts towards beam **2** (or **1**) with an intensity of I_{01}. The diffraction efficiency is determined as follows:

$$\eta = 100\frac{I_{01}}{I_{01}+I_3'},$$

where I_3' is the intensity of the non-distorted readout beam passed through the photorefractive layer under diffraction. A salient feature of the PR media is the possibility of fast writing dynamical holograms with $\eta \approx 100\%$ (the writing time is of the order of several milliseconds).[31–34] It should be noted that the diffraction efficiency contains no information on the phase shift of the grating relative to the fringe pattern. Below we will consider creation of a grating with a zero phase shift in the system exhibiting both photoelectric and nonlinear optical properties.[34] Therefore, only analysis of the kinetic curves for two-beam coupling with amplification of one beam at the attenuation of the other beam (see Fig. 3) provides an unambiguous proof of the PR effect.

III. The figure of merit of nonlinear optical chromophores

Choosing a chromophore involves estimation of its Figure of Merit (FOM), which characterises the ability of the chromophore to generate the PR effect.[15,35–41] Criteria for choosing chromophores with high FOM have been reviewed.[15] Photorefraction in inorganic crystals is primarily due to the Pockels electro-optic effect; therefore, in this case one deals with the FOM_{PEO}.[4] As to the polymeric media, the Δn_{PEO} and Δn_{KEO} and Δn_{OB} parameters can contribute largely to the refractive index modulation. In the case of non-plasticised high-T_g polymeric systems containing low-molecular-mass chromophores with small FOM_{KEO} after alignment of the chromophores in the field E_p the refractive index modulation Δn is due to the Pockels electro-optic effect only and here we have to deal with

$$FOM_{PEO} = \frac{\beta\mu_g}{M},$$

where M is the molecular mass. Generally, various polarisation mechanisms of nonlinear optical chromophores[35–40] contribute to the refractive index modulation

$$[FOM] = FOM_{OB} + FOM_{PEO} + FOM_{KEO}.$$

Combining different contributions of the polarisation to the overall FOM requires the appearance of some constants in addition to the corresponding molecular characteristics; therefore, the FOM in the case of low-molecular-mass chromophores (FOM_{KEO} is negligible) is given by the following relationship[15,16,39,40]

$$[FOM] = \frac{1}{M}\left[2\Delta\alpha(0)\frac{\mu_g^2}{kT} + 9\mu_g\beta(0)\right].$$

The figure of merit depends on the degree of charge transfer δ in the nonlinear optical chromophore.[35–41] Indeed, the molecule of such a chromophore incorporates an electron-donor (D) and an electron-acceptor (A) group linked by a system of conjugated bonds, $D^{+\delta}-Sp-A^{-\delta}$ (Sp is a spacer). The structural formulae of some of the most widely used chromophores are presented below. The degree of charge transfer is determined by the contributions of two resonance structures, without (D–Sp–A) and with full charge transfer ($D^{+1}-Sp-A^{-1}$), to the ground state[42]

$$D^{+\delta}-Sp-A^{-\delta} = a(D-Sp-A) + b(D^{+1}-Sp-A^{-1}), \quad (17)$$

where

$$\delta = \frac{b^2}{a^2+b^2} = c^2.$$

When choosing an optimum chromophore, one should study how the contributions of various FOMs depend on the mixing parameter (c^2 parameter, MIX) of these two structures.[38,40,41] As parameter is also given the bond length alternation in the conjugated molecule[35,43–46] (namely, the difference, Δr, between the average lengths, r, of the single and double carbon–carbon bonds, which in turn depends on the degree of charge transfer in the chromophore). The orientational polarisability is positive at any Δr value. According to Marder *et al.*,[44] the bond lengths in polyenes ($c^2 = 0$) are as follows: $r(C-C) = 1.45$, $r(C=C) = 1.34$ and $\Delta r = 0.11$ Å. Introduction of the D and A groups causes an increase in c^2 and a decrease in the Δr value; in this case β and the third-order molecular polarisability (γ) are positive. At $c^2 = 0.5$, the bond lengths equilibrate ($\Delta r = 0$); *i.e.*, the molecular structures become symmetric (the so-called cyanine limit). At this degree of charge transfer, $\beta = 0$ while γ reaches its maximum negative value. On going to zwitterionic structures at $c^2 > 0.5$ the Δr and β values become negative. As a consequence, the Δn_{OB} and Δn_{PEO} parameters of this type of chromophore have opposite signs.

Photoexcitation of a chromophore containing the D and A groups causes a change in the degree of charge transfer from δ to $1-\delta$ due to electron transfer (see Ref. 42)

$$D^{+\delta}-Sp-A^{-\delta} \xrightarrow{h\nu} D^{1-\delta}-Sp-A^{-1+\delta}.$$

Here $h\nu = E_{ge}$. The ground-state and excited-state dipole moments of the chromophore are respectively

$$\mu_g = e\delta r_{DA},$$

$$\mu_e = e(1-\delta)r_{DA},$$

where e is the charge of an electron and r_{DA} is the distance between the D and A groups. Thus, the difference

$$\Delta\mu = \mu_e - \mu_g$$

approaches μ_e at $\delta \approx 0$, decreases down to zero for centrosymmetric chromophores ($\delta = 0.5$) and becomes negative at $\delta > 0.5$.

Numerous studies on the 'guest–host' photorefractive polymeric systems containing dipole chromophores have been reported.[4,12] As mentioned above, alignment of chromophores in the bulk of high-T_g polymers requires the prepoling in a constant field E_p at a temperature T_p, which is 2 to 20 °C higher than T_g.[41] On subsequent cooling of the system below T_g in the presence of the polarising field E_p the chromophore alignment is 'frozen'.

It should be noted that, depending on the properties of the polymer matrix, 'unfreezing' of rotational diffusion can occur at temperatures much below T_g. For instance, the intensity of the second laser harmonic generated in a poly(methyl methacrylate) (PMMA) layer doped with poly(ethylene oxide) and nonlinear optical chromophore 4-anilino-4′-nitroazobenzene (DO-3 dye) substantially increases after heating of the system at 52–57 °C and reaches the same values as those obtained after heating at temperatures above T_g (92–95 °C).[47] This effect is due to an increase in the volume expansion coefficient of the polymer blend in the temperature range 52–57 °C.[48]

After alignment of the oligomeric chromophores in the E_p field the refractive index modulation is due to the Pockels and Kerr electro-optic effects. If we go to the molecular polarisabilities, formula (7) takes the form [41]

$$\Delta n_1 = \Delta n_{PEO} + \Delta n_{KEO} = \tag{18}$$

$$= \frac{2\pi}{n}\frac{Nf^2(0)f(\omega)E_{sc}}{5}\left[\beta(-\omega,\omega,0)\frac{\mu_g E_p}{kT_p} + \gamma(-\omega,\omega,0,0)E_0\right],$$

where

$$\beta(-\omega,\omega,0) = \beta(0)\frac{E_{ge}^2\left[3E_{ge}^2 - (h\omega)^2\right]}{3\left[E_{ge}^2 - (h\omega)^2\right]^2},$$

$\omega = 2\pi/\lambda$, λ is the laser wavelength at which the PR effect is measured and $\beta(0)$ is the static contribution to the second-order molecular polarisability extrapolated to $h\omega = 0$.[7, 16–19] The two-level polarisation model [14] defines the molecular polarisabilities as follows:

$$\beta(0) = \frac{6\mu_{ge}^2\Delta\mu}{E_{ge}^2}, \tag{19}$$

$$\gamma(0) = \frac{24(\Delta\mu^2 - \mu_{ge}^2)\mu_{ge}^2}{E_{ge}^3} + \frac{24\mu_{ge}^2\mu_{ee'}^2}{E_{ge'}E_{ge}^2},$$

where $\Delta\mu = \mu_e - \mu_g$, $\mu_{ee'}$ is the dipole moment of the transition from the first to the second excited level and $E_{ge'}$ is the energy of transition from the ground state to the second excited state.[43–46, 49]

Taking into account the net FOM, formula (18) can be written as follows:

$$\Delta n_1 = \Delta n_{PEO} + \Delta n_{KEO} = \frac{2\pi}{n}\frac{Nf^2(0)f(\omega)E_p}{5kT_p}[\text{FOM}],$$

where

$$[\text{FOM}] = \text{FOM}_{PEO} + \text{FOM}_{KEO} = \mu_g\beta(0) + \frac{E_0kT_p}{E_p}\gamma(0), \tag{20}$$

where E_0kT_p/E_p is a constant.

At room temperature, anisotropic chromophores in low-T_g polymers are in the mobile state and can be aligned during measurements of the PR effect in the E_t field, which changes both its direction and amplitude (see Fig. 2*b*). In this case a doubled FOM_{PEO} value is introduced into Eqn (20) (see Refs 35, 40, 41, 45)

$$[\text{FOM}] = \text{FOM}_{PEO} + \text{FOM}_{KEO} = 2\mu_g\beta(0) + kT\gamma(0). \tag{20a}$$

As mentioned above, the refractive index modulation arises in the low-T_g polymeric composites due to the linear orientation polarisation of a dipole chromophore in the E_t field. Therefore, the expression for the net refractive index modulation must contain an additional term Δn_{OB} [see formula (8)]

$$\Delta n = \Delta n_{OB} + \Delta n_{PEO} + \Delta n_{KEO} = \tag{21}$$

$$= \frac{4\pi}{n}\frac{Nf^2(0)f(\omega)E_t^2}{45kT}[\text{FOM}],$$

where

$$[\text{FOM}] = \text{FOM}_{OB} + \text{FOM}_{PEO} + \text{FOM}_{KEO},$$

$$\text{FOM}_{OB} = \frac{\Delta\alpha(0)\mu_g^2}{kT}.$$

Since the net modulation, Δn, is quadratically dependent on E_t, it was assumed [15, 16, 39, 40] that creation of a grating in low-T_g composites is due to the Kerr electro-optic effect only. By substituting Eqn (20a) into relationship (21) we get

$$[\text{FOM}] = \text{FOM}_{OB} + \text{FOM}_{PEO} + \text{FOM}_{KEO} = \tag{21a}$$

$$= \Delta\alpha(0)\frac{\mu_g^2}{kT} + 9\mu_g\beta(0) + \frac{9}{2}kT\gamma(0).$$

This expression is, as a rule, used when comparing the contributions of various polarisation mechanisms to the amplitude of the refractive index modulation.[41]

To prepare photorefractive polymeric systems, chromophores possessing the maximum net FOM are chosen. The parameters in formula (21a) are determined from ellipsometric measurements, by analysing the optical and electro-optical absorption spectra in solution [15, 16, 39–41] and from quantum-chemical calculations.[35–38, 43–46]

1. Photorefractive polymeric systems with low glass transition temperatures

The FOM values of typical chromophores used in studies of the PR effect are listed in Table 1. When choosing nonlinear optical chromophores for photorefractive composites based on both low- and high-T_g polymers, these data allow estimation of the relative contributions of various polarisation mechanisms to the creation of a phase grating using formulae (20) and (21a). As can be seen, for all chromophores

$$\text{FOM}_{OB} \gg \text{FOM}_{PEO} + \text{FOM}_{KEO},$$

i.e., low-T_g polymers must have a much higher refractive index modulation and, hence, PR-characteristics than the samples with high T_g.

Analysis of the data listed in Table 1 also reveals that if chromophores incorporated into high-T_g polymers (in this case $[\text{FOM}] = \text{FOM}_{PEO} + \text{FOM}_{KEO}$) are preliminarily aligned in the E_p field at $T_p \gg T_g$, the Pockels electro-optic effect makes major contribution to the creation of a grating. Otherwise the phase grating amplitude in high-T_g polymeric systems is determined only by the Kerr electro-optical coefficient whose contribution to the net FOM allows one to assume that the PR-characteristics, *e.g.*, Γ [see formula (12)] should be much lower than the corresponding characteristics obtained for polymer composites with low T_g.

Since 1994 (see Ref. 10), the vast majority of photorefractive materials were synthesised using polymers with glass transition temperatures close to room temperature. Most of them are based on plasticised poly(vinylcarbazole) (PVCz),[12, 19, 31–33, 50–54] carbazolyl-substituted polysiloxanes (PSX-Cz) [55–57] and polyethers.[58, 59] In such polymeric media the major contribution to the creation of a phase grating comes from the linear orientation polarisation. Under these conditions, the diffraction efficiency buildup rate is determined by rotational diffusion of the chromophore and is described as follows:[60, 61]

$$\eta(t) \sim \sin^2\left[A_1\left(1 - e^{-D_1t}\right) + A_2\left(1 - e^{-D_2t}\right)\right],$$

where

$$A_1 + A_2 = \frac{\pi}{2},$$

and D_1 and D_2 are coefficients: $D_n = n(n+1)D$ at $n = 1$ and 2; and D is the rate constant for rotational diffusion.

Table 1. Figure-Of-Merit values (in 10^{-46} e.s.u.) for chromophores of various structure.

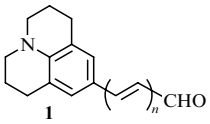
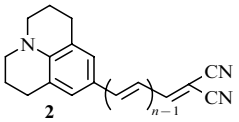
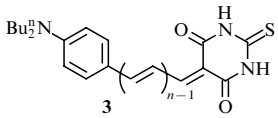
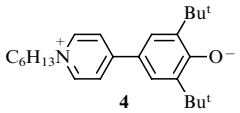
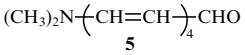
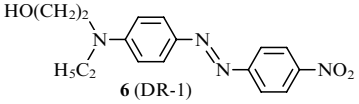
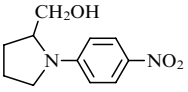
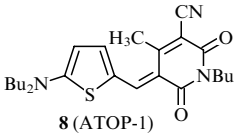
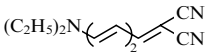
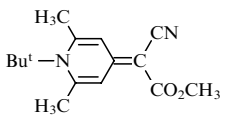
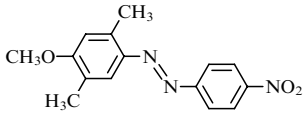
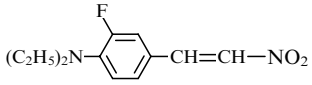
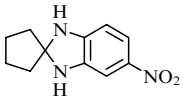
Chromophore		Solvent	FOM_{PEO} (see [a])	FOM_{KEO} (see [a])	FOM_{OB} (see [a])	[FOM]	$\frac{FOM_{OB}}{[FOM]}100$ (%)	Ref.
formula	*n*							
 **1**	1	dioxane	32	2.2	180	214	84	41
	2	"	50	4.5	216	270	80	41
	3	"	130	18	378	528	71.6	41
 **2**	1	"	63	4.5	576	639	90	41
	2	"	170	9	810	989	82	41
	3	"	280	41	1229	1550	79.3	41
	4	"	540	68	1548	2156	72	41
	5	"	1233	189	2341	3763	62	41
 **3**	1	"	86	−2.25	545	629	86.6	41
	1	chloroform	110	–	810	920	88	37
	2	dioxane	274	9	1161	1444	80.4	41
	2	chloroform	295	–	1400	1695	82.6	37
	3	dioxane	549	76.5	1305	1930	67.6	41
	3	chloroform	630	–	2335	2965	78.8	37
	4	dioxane	927	184.5	1710	2821	60.6	41
	4	chloroform	1070	–	2920	3990	73.2	37
	5	dioxane	1800	580	2254	4634	48.6	41
	5	chloroform	2190	–	3270	5460	60	37
 **4**		"	–	–	970	–	–	38
		dioxane	−2.5	–	1500	–	–	38
		THF	−50	–	1640	1590	103	38
		chloroform	−50	–	2105	2055	102	38
		acetone	−100	–	2205	2105	104	38
		DMSO	−170	–	3015	2845	106	38
		methanol	−160	–	2885	2725	106	38
 **5**		see [b]	–	–	530	–	80	35
 **6** (DR-1)		chloroform	486	–	1620	2106	77	36
 **7** (NPP)		"	54	–	380	435	87.4	36
 **8** (ATOP-1)		dioxane	45	−9	2354	2390	98.5	41
 **9** (DCDEAHT)		"	90	−4.5	1431	1516	94.4	41
 **10** (DHP)		see [b]	–	–	530	–	99.3	39

Table 1 (continued).

Chromophore formula	*n*	Solvent	FOM_{PEO} (see [a])	FOM_{KEO} (see [a])	FOM_{OB} (see [a])	[FOM]	$\frac{FOM_{OB}}{[FOM]}100$ (%)	Ref.
 **11** (DMNPAA)		see [b]	–	–	285	–	88.1	39
 **12** (FDEANST)		"	–	–	357	–	75.4	39
 **13** (DTNBI)		"	–	–	350		87.4	39

[a] $FOM_{PEO} = 9\mu_g\beta(0)$, $FOM_{KEO} = 9kT\gamma(0)/2$ and $FOM_{OB} = \Delta\alpha(0)\mu_g^2/kT$ [see formula (21a)]. [b] Obtained from quantum-chemical calculations.

The determining role of plasticiser was demonstrated taking composites prepared from carbazolyl-substituted polysiloxane, 2,4,7-trinitro-9-fluorenone (TNF) and indole derivatives (chromophores) as examples. The major contribution (97%) to the net FOM of this system comes from the FOM_{OB}.[57] In the absence of plasticiser this composite has $T_g = 34$ °C and the net internal gain $(\Gamma - \alpha)$ is close to 2 cm^{-1}. Doping with a small amount of plasticiser (ethylcarbazole, ECz) causes lowering of the T_g value down to 23 °C and an increase in $(\Gamma - \alpha)$ to 25 cm^{-1} (see Ref. 57). The steady-state value of the net internal gain is achieved about 1 s after the start of two-beam coupling, which is believed to correspond to the reorientation time of nonlinear optical chromophores in the E_t field. It was also pointed out [62] that nonlinear optical chromophores form aggregates, which cannot be oriented in the applied field E_0; as a consequence, the PR effect is weakened. For this reason, the side butyl groups are introduced into the chromophore molecule (see Table 1, compound **8**) to preclude dimerisation.

2. Photorefractive polymeric systems with high glass transition temperatures

The data for compound **2** (see Table 1) show that an increase in the number of conjugated bonds from 1 to 5 causes a respective increase in the FOM_{PEO} and FOM_{KEO} values by a factor of 19.6 and 42. The third-order molecular polarisability of acetylene oligomers with the number of conjugated bonds varying from $n = 1$ to 31 increases with an increase in the length of the conjugated system as follows:[49, 63–65]

$$\gamma(0) = \gamma_1(0)n^{2.5\pm0.2}. \quad (22)$$

J-Aggregates of cyanine dyes are known to have a very high third-order susceptibility.[66–69] The corresponding dependence

$$\chi^{(3)} \sim n^{2.36},$$

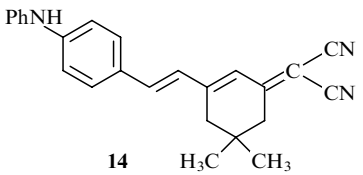
coincides with relationship (22) within the limits of experimental error. The third-order volume susceptibility, $\chi^{(3)}$, of J-aggregates of dyes can be as high as nearly 2.7×10^{-13} C m J^{-3} (in SI units).[66] This value is due to co-operative electronic excitation of molecules and delocalisation of the excitation along the whole length of the J-aggregate, which comprises n conjugated bonds.[66–69] Orientational diffusion of dipole chromophores in high-T_g polymers is restricted; therefore, after application of the field E_t the major contribution to the refractive index modulation [see Eqns (21) and (21a)] should be expected only from the third-order electronic polarisation. It is the use of J-aggregates of cyanine dyes as nonlinear optical chromophores that allowed the obtention of high PR-characteristics of composites based on aromatic polyimide with $T_g \approx 230$ °C,[29, 30] which are comparable with the corresponding parameters of plasticised composites based on PVCz.

Poly(diacetylenes) [49, 70–72] and polyenes of various structures [73] are also characterised by rather high $\chi^{(3)}$ values; however, they are several orders of magnitude lower than those of J-aggregates.

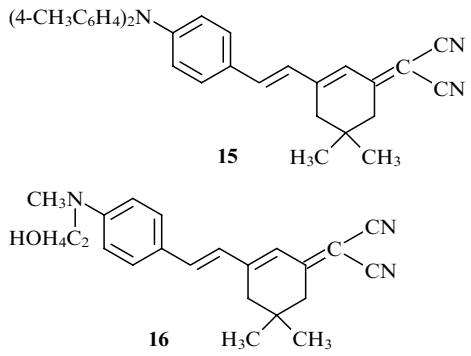
IV. Interrelation between the photorefractive effect and the photoelectric and electron transport properties

Depending on the composition of a system, the PR-characteristics can be related in a different manner to the rate of charge photogeneration, charge carrier mobility or to the rate of rotational diffusion of a nonlinear optical chromophore in the field E_t. When creating dynamical holograms, it is essential to achieve a short response time of the polymer layer to the two-beam coupling. Therefore, it seems likely that polymeric systems with electronic polarisation rather than orientational effects, which are limited to rotational diffusion of the chromophore in the matrix, should be more promising in this case.

Note that the ionisaton potential of the chromophore (I_D) influences the high two-beam coupling gain coefficients and diffraction efficiency more strongly than the nonlinear optical characteristics responsible for the FOM values.[33, 74] This was established taking composites prepared from PVCz containing the donor carbazolyl groups (Cz), acceptor (2,4,7-trinitro-9-fluorenylidene)malonodinitrile (TNFDM) and the chromophores **14**–**16** as examples.



14



The donor–acceptor complex PVCz·TNFDM is responsible for the photoelectric sensitivity of these composites. The ionisaton potentials of the carbazolyl group, Cz, and chromophores **14**–**16**, their FOM values, and the most important PR-characteristics of the composites are listed in Table 2. The refractive index modulation Δn_{max} was estimated from the the η values measured in the presence of chromophores **14**–**16** using formula (16), which was modified to include the sample geometry and had the form [33, 74]

$$\eta = \sin^2(586\,\Delta n_{max}).$$

The product $\Delta n_{max}\sin\psi$ was calculated using the measured two-beam coupling gain coefficients Γ and formulae (15) and (12a). Therefore, by comparing η and Γ it is possible to determine the phase shift ψ (see Table 2), which decreases in the series of the chromophores **14**–**16**. Analysis of the measured η values showed that the Δn_{max} values increase by a factor of 1.6 and 2.2 if the chromophore **14** is replaced by **15** and the chromophore **15** is replaced by **16**, respectively. Taking into account the fact that these replacements cause a much smaller increase in the FOM value (by a factor of 1.06 and 1.2, respectively), it was concluded that the Δn_{max} value is primarily determined by the space-charge field E_{sc} rather than FOM (the larger the ionisaton potential difference between the carbazolyl group and the nonlinear optical chromophore, the stronger the E_{sc} field). It was hypothesised [33, 74, 75] that the increase in E_{sc} is due to an increase in the quantum yield of holes, which can be related to the hole jump to chromophore (Ch) during the reactions

$$\text{PVCz}\cdot\text{TNFDM} \overset{h\nu}{\rightleftharpoons} \text{PVCz}^{+\bullet}\cdots\text{TNFDM}^{-\bullet}, \quad (23)$$

$$\text{PVCz}^{+\bullet} + \text{Ch} \longrightarrow \text{PVCz} + \text{Ch}^{+\bullet}. \quad (23a)$$

Hole jump to chromophore by reaction (23a) precludes its disappearance *via* recombination of the radical ion pair following reaction (23), thus increasing the quantum yield of holes. The molecules of acceptor, TNFDM, act as deep electron traps; therefore they persist in the region of bright fringes. When present in low concentrations, chromophores act as hole traps; however, at high concentrations (28.5% of the composite mass) they serve as charge transport agents [33, 74, 75]

Table 2. Ionisaton potentials and FOM values for chromophores **14**–**16** and the most important characteristics of polymeric photorefractive composites based on PVCz,[a] TNFDM and chromophores **14**–**16** at 60 V μm^{-1} (see Refs 33 and 74).

Chromophore	I_D /eV	FOM (rel.u.)	Composite characteristics		
			η (%)	Γ /cm^{-1}	ψ /deg
14	5.59	1.0	25	70	37
15	5.46	1.06	40	88	29
16	5.40	1.27	85	167	25

[a] The ionisaton potential of the carbazolyl group is 5.90 eV.

$$\text{Ch}^{+\bullet} + \text{Ch} \longrightarrow \text{Ch} + \text{Ch}^{+\bullet}.$$

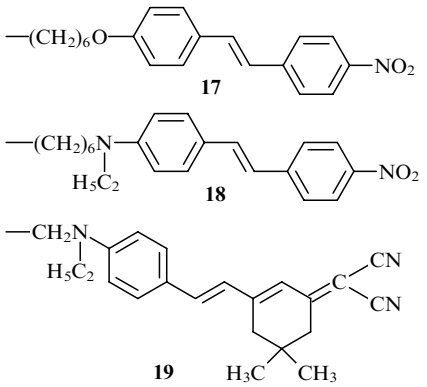
The photoconductivity and the quantum yield of mobile holes in the composite prepared from PVCz, sensitiser (TNFDM), plasticiser (ECz) and a nonlinear optical chromophore were shown [75] to increase by nearly an order of magnitude upon replacement of TNFDM by C_{60} fullerene. This is due to the corresponding decrease in the probability of recombination of charge carriers by reaction (23).

The larger the difference

$$\Delta I_D = I_D(\text{Cz}) - I_D(\text{Ch}),$$

the higher the probability that efficient deep hole traps will be formed.[33, 74, 75] Therefore, a decrease in I_D(Ch) causes shortening of the hole path length and a corresponding decrease in the phase shift ψ (see Table 2). The limiting case, *viz*., a decrease in phase ψ down to zero was found for a composite prepared from PVCr, TNF (acceptor) and nonlinear optical chromophore 2-(4-nitro-henyl)-4,5-bis(4-methoxyphenyl)imidazole (Lophine-1, 33 mass %) (see Ref. 34). The effect is due to the fact that, similarly to an electron, a hole trapped by the chromophore by reaction (23a) remains immobile in the region of bright fringes and, hence, no PR effect occurs. The formation of a Lophine-1$^{+\bullet}\cdots$TNF$^{-\bullet}$ radical ion pair is accompanied by the appearance of the corresponding band in the optical absorption spectrum and changes the layer composition, thus causing creation of the amplitude and phase gratings with zero phase shift ($\psi = 0$), similarly to conventional photochemical writing of a hologram.

In poly(methyl methacrylate) with carbazolyl-containing side groups and the chromophores **17**–**19**,



the T_g value was changed by introduction of different amounts of liquid-crystalline plasticiser 4-$C_7H_{15}C_6H_4C(O)OC_6H_4CN$-4. It was found that the larger the $T_e - T_g$ difference (T_e is the temperature of the experiment), the higher the photoconductivity and the phase shift ψ. It was concluded that raising the temperature causes an increase in the hole path length (until trapping by deep traps), which in turn leads to an increase in ψ. If at a constant temperature of the experiment (T_e = 21 °C) the ($T_e - T_g$) difference increased due to a decrease in T_g caused by an increase in the concentration of plasticiser, Γ increased more slowly than η.[76] This is due to a decrease in the phase shift ψ as a result of reduction of the mobility of charge carriers on dilution of carbazolyl transport groups with neutral plasticiser molecules. Experiments with a composite prepared from PVCz, TNF and the nonlinear optical chromophore *N*,*N*-diethyl-*p*-nitroaniline (EPNA) and doped with 4-(diethylamino)benzaldehyde diphenylhydrazone (DEH) showed that the phase shift depends on the dopant concentration in a complex manner. The ionisaton potential of DEH is somewhat lower than that of PVCz.[77] Comparison of the Γ and η values obtained at 633 nm revealed that $\psi = 32°$ for the undoped material, decreases to 8° upon doping with about 2×10^{-3} mass % of DEH and down to nearly zero at 2 mass % of DEH but then increases and reaches a value of 45° at a DEH

concentration of 20 mass %. The effect is due to the fact that photogenerated holes, which did not undergo recombination by reaction (23), migrate from one carbazolyl group of PVCz to another by the hopping mechanism

$$PVCz^{+\cdot} + PVCz \longrightarrow PVCz + PVCz^{+\cdot}. \qquad (23b)$$

When present in low concentrations, the DEH molecules act as traps of mobile holes

$$PVCz^{+\cdot} + DEH \longrightarrow PVCz + DEH^{+\cdot}$$

and thus restrict the free path of charge carriers. However, as the DEH content increases to ~ 8 mass % and the average distance between neighbouring molecules is correspondingly shortened, they provide hole transportation by the hopping mechanism

$$DEH^{+\cdot} + DEH \longrightarrow DEH + DEH^{+\cdot}.$$

In a composite prepared from PVCz, TNF and the nonlinear chromophore 1-(2′-ethylhexyloxy)-2,5-dimethyl-4-(4″-nitrophenylazo)benzene the chromophore molecules also play the role of hole traps at low concentrations but become responsible for hole transportation in the PR layers if the chromophore concentration reaches 47.5 mass %. Under these conditions the hole mobility (2×10^{-6} cm^2 V^{-1} s^{-1}) remains unchanged upon replacement of the PVCz matrix by the dielectric polycarbonate matrix.[78]

The grating buildup speed can be related to the quantum yield of charge carriers (φ) and to the time it takes for a charge carrier (t_{tr}) to travel the distance $\Lambda/2\cos\phi$ as follows:

$$\frac{\partial E_{sc}}{\partial t} \sim \frac{\partial N_h}{\partial t} = \frac{\varphi I_0(1-10^{-A})\lambda 2\cos\theta}{\Lambda hc} - \frac{N_h}{t_{tr}}, \qquad (24)$$

where $\Lambda/2\cos\phi$ is the distance from the bright fringe to the midpoint between the interference-maximum regions along the direction of the E_0 field (see Fig. 2 *a*); N_h is the concentration of the photogenerated holes determining the photocurrent j_{ph}; I_0 is the laser light intensity; $(1-10^{-A})$ is the fraction of light energy absorbed within the layer (A is the optical absorption); and hc/λ is the light quantum energy. Formula (24) was derived assuming $\psi = \pi/2$; *i.e.*, the hole distribution in Fig. 2 *b* is centred at the midpoint between the bright fringes.

In the API-based composites containing J-aggregates of carbocyanine dyes the free carrier generation rate determines the kinetic characteristics of photorefraction, as demonstrated by analogy between the kinetic curves for the growth of photocurrent (Fig. 4) and the kinetic curves for two-beam coupling (see Fig. 3).[29, 30, 79, 80] The curve for the growth of photocurrent measured for the API/Dye 1 composite (see Fig. 4 *a*) is described by a biexponential dependence

$$\frac{j_{ph}+j_d}{j_d} = 14 - 7\exp\left(-\frac{t}{3}\right) - 6\exp\left(-\frac{t}{45}\right)$$

with the time constants $\tau = 3$ and 45 s. In the case of two-beam coupling (see Fig. 3 *a*) the intensity $I_2(L)_t$ increases synchronously with the fast component of photocurrent

$$\frac{I_2(L)_t}{I_2(L)_{t=0}} = 1 + 0.125\left[1 - \exp\left(-\frac{t}{3}\right)\right]$$

(time constant $\tau = 3$ s). The diffraction efficiency also increases with the time constant $\tau = 3$ s. Thus, in these composites the rate of hole accumulation, $\partial N_h/\partial t$, determines the time constant for the growth of the intensity $I_2(L)_t$. This is additionally confirmed by the correspondence between the rapid increase in the gain coefficient $I_2(L)_t/I_2(L)_{t=0}$ for the API/Dye 2 composite, for which $\tau < 20$ ms (see Fig. 3 *b*), and the equally rapid appearance of a steady-state photocurrent as the laser is switched on (see Fig. 4 *b*). In this case the speed of writing of the grating can be limited by the mobility of charge carriers μ. The available data on the mobility of charge carriers in composites of close compositions show that

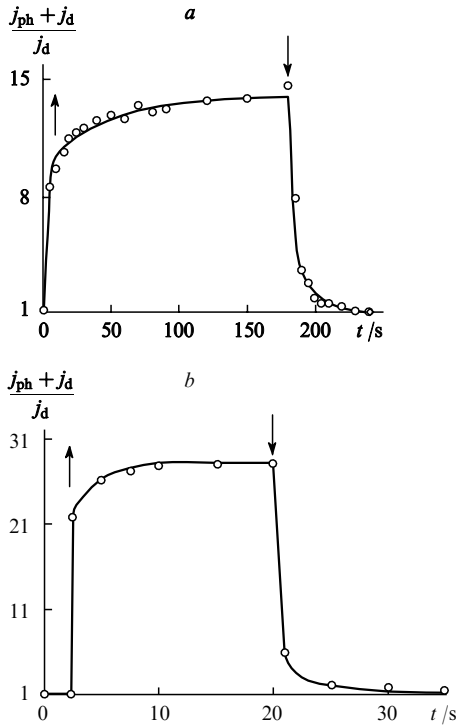


Figure 4. Changes in the $(j_{ph} + j_d)/j_d$ ratio (j_d is the dark current) for the API/Dye 1 (*a*) and API/Dye 2 (*b*) composites upon switching an Ar–Kr-laser beam (647 nm, $I_0 = 0.06$ W cm^{-2}) on (upward arrow) and off (downward arrow).[79, 80]

$\mu \approx 10^{-4}$ cm^2 V^{-1} s^{-1} (see Refs 81 and 82); this allows one to conclude that the time a charge carrier takes to travel a distance $\Lambda/2\cos\phi$ ($\Lambda = 1653$ nm) is

$$t_{tr} = \frac{\Lambda}{2E_0\mu\cos\phi}. \qquad (25)$$

At $E_0 = 16$ V μm^{-1}, the time t_{tr} is $\sim 6 \times 10^{-6}$ s, which is much shorter than the response time ($\tau = 3$ s) to the two-beam coupling (see Fig. 3 *a*).

It should be noted that if the photocurrent is measured under conditions corresponding to attainment of the steady-state value $(j_{ph} + j_d)/j_d$, *i.e.*, when $\partial N_h/\partial t = 0$ in Eqn (24), deep traps are filled and the lifetime of the photogenerated charge carriers is not trap-limited. Since the photoconductivity is related to the photocurrent as follows

$$\sigma_{ph} = \frac{j_{ph}}{E_0} = N_h e\mu,$$

at $\partial N_h/\partial t = 0$ formula (24) can be rewritten so that it allows estimation of the quantum yield of mobile charge carriers (photogeneration efficiency)

$$\varphi = \frac{j_{ph}hc}{e\lambda I_0(1-10^{-A})}. \qquad (26)$$

The efficiency of photogeneration of transportation centres, measured using the field dependence of the photocurrent, coincided with the efficiency estimated using the xerographic discharge curves. In the latter case no negative electrode was available and φ was determined from the rate of disharge of the surface potential, V_0, which appeared upon deposition of negatively charged CO_3^- ions formed in the corona discharge in air near the surface of the layer on the free surface of the polymer

layer. The parameter $(dV/dt)|_{V_0}$ was estimated at different V_0 values from the difference

$$\left.\frac{dV}{dt}\right|_{V_0} = \left.\frac{dV}{dt}\right|_{V_0\,(\text{light})} - \left.\frac{dV}{dt}\right|_{V_0\,(\text{dark})},$$

where $(dV/dt)|_{V_0\,(\text{light})}$ and $(dV/dt)|_{V_0\,(\text{dark})}$ are the initial fall-off rates of the surface potential upon switching on the light and in the dark, respectively. In contrast to the method involving measurements of the field dependence of the photocurrent (the steady-state photocurrent value is attained after full occupation of deep traps, see above), xerography allows measurements of φ with empty traps. The quantum yield of charge carriers is proportional to the initial potential drop $(dV/dt)|_{V_0}$

$$\varphi(V) = \frac{\varepsilon\varepsilon_0 hc}{e\lambda I_0(1-10^{-A})d}\left.\frac{dV}{dt}\right|_{V_0}. \qquad (26a)$$

The $j_{ph}(E_0)$ dependence measured in the API/Dye 1 composites has the form [79, 80]

$$j_{ph} = a(E_0)^{3.5}, \qquad (27)$$

where a is a constant. In accordance with this relationship the photoconductivity,

$$\sigma_{ph} = \frac{j_{ph}}{E_0},$$

and the photoelectric sensitivity (photoconductivity per unit of light intensity),

$$S = \frac{\sigma_{ph}}{I_0},$$

depend on the field E_0

$$\sigma_{ph} = a(E_0)^{2.5},$$

$$S = \frac{a(E_0)^{2.5}}{I_0}.$$

The field dependence of the quantum yield of mobile charge carriers [see Eqn (26)] is also described by a power function

$$\varphi = b\varphi_0(E_0)^{3.5}. \qquad (28)$$

Here b is a constant and φ_0 is the quantum yield of the bound, isolated and thermalised electron–hole pairs with the initial electron–hole distance r_0. To estimate the φ_0 and r_0 values, the probability that the electron–hole pair escapes recombination was calculated using the Onsager equations for Brownian motion of charges in the field E_0 with inclusion of the Coulombic attraction. Since the experimental field dependence of φ is linear in the $\varphi-(E_0)^{3.5}$ coordinates, a method for solving the Onsager equations expanded of up to the $(E_0)^4$ term [83] was employed.

Figure 5*a* presents the quantum yield, φ, of mobile charge carriers plotted *vs.* the applied field E_0 determined from the photocurrent for the API/Dye 1 composite. The curve calculated using the Onsager equation at $\varphi_0 = 0.2$ and $r_0 = 12$ Å fits well the experimental points. As can be seen in Fig. 5*b*, the experimental φ values estimated both from the photocurrent [see Eqn (26)] and xerographically [see Eqn (26a)] virtually coincide. This is due to the fact that for both experimental methods trapping by deep traps imposes no limitations on the lifetime of photogenerated charge carriers, since, as mentioned above, in the former case they are fully occupied while in the latter they are empty and the measurement time is shorter than the trapping time of the charge carriers. It should be noted that Melz [84] related the parameter r_0 to the exponent, m, in the formula

$$\varphi = b\varphi_0(E_0)^m$$

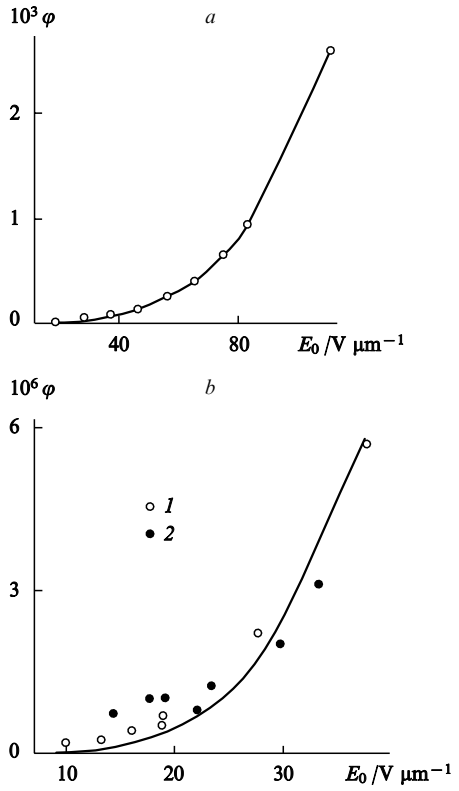


Figure 5. Quantum yield (φ) *vs.* E_0 plot for the API/Dye 1 composite: overall curve (*a*) and its initial portion (*b*).[79, 80]
(*a*) φ values were estimated from photocurrent using formula (26) (points); (*b*) φ values were estimated from the photocurrent using formula (26) (*1*) and from xerographic curves using formula (26a) (*2*); solid lines were obtained from calculations using the Onsager formula with $\varphi_0 = 0.2$ and $r_0 = 12$ Å.

at $\varepsilon = 3$ and $T = 23$ °C using the Onsager theory. He also found that if the distance between charge carriers is ~12–13 Å, $m = 3.5$. Thus, the r_0 value obtained [79, 80] with this m coincides with the calculated value.

Detailed analysis of the studies on charge photogeneration and transport in polymeric systems can be found in some monographs (see, *e.g.*, Refs 85 and 86).

The linear dependence φ on the applied field was obtained for the polysiloxane PR layers bearing side carbazolyl groups (PSCz) and doped with trinitrofluorenone and the chromophores FDEANST or DTNBI.[87] The hole mobility in these layers is nearly 2×10^{-7} cm^2 V^{-1} s^{-1} at $E_0 = 16$ V μm^{-1}. Estimation using formula (25) showed that the time taken to travel the distance $\Lambda/(2\cos\phi)$ is 1–2 ms, which is nearly 100 times shorter than the experimentally determined time constant for the growth of the signal beam intensity.[88] It seems likely that in this polymeric system the rate of photogeneration charge also determines the speed of writing of the grating.

The mobility of charge carriers in the PR composites comprised of a polystyrene matrix, the nonlinear optical chromophore 2,2-dimethyl-4-(4-nitrophenylazo)phenol and various low-molecular-mass transport dopants is reduced by more than two orders of magnitude as the dipole moment of the dopant molecules increases from 1 to 4 D.[88] The highest mobility (4×10^{-6} cm^2 V^{-1} s^{-1}) at 16 V μm^{-1} was obtained for hole transport with 1,1-bis(di-4-tolylaminophenyl)cyclohexane while the lowest one (2×10^{-8} cm^2 V^{-1} s^{-1}) was obtained for electron transport along the 1,1′-dioxo-2-(4-methylphenyl)-6-phenyl-4-(dicyanomethylidene)thiopyran molecules. Such a change in the mobility corresponds to extension of the t_{tr} time from 1 to 200 ms; in the latter case the speed of writing of the grating can be limited

by transport of charge carriers. To identify the stage responsible for the speed of writing, the kinetic curves of the growth of the diffraction efficiency in the PVCz/TNF/DMNPAA system doped with high concentration of plasticiser (ethylcarbazole, T_g = 10 °C) were measured under different writing conditions.[89] The efficiency $\eta = 0.85\,\eta_{max}$ was observed after 73.2 s if both beams were switched on and then the E_0 field was switched on and after 2.18 – 5.54 s if the E_0 field was switched on 30 min before switching on both beams. Such a shortening of the response time was associated with the fact that chromophores pre-oriented in the E_0 field are only slightly reoriented as E_{sc} increases and that this reorientation occurs much faster than reorientation from the disordered state.

The dependence $j_{ph} \sim E_0^m$ corresponding to the Onsager theory is masked in the presence of ionic components. Indeed, in contrast to the systems considered above experiments with poly(phenylenevinylene) containing sensitisers, tri(bipyridyl)ruthenium complexes $Ru(bipy)_3^{2+}(PF_6^-)_2$, and fragments with nonlinear optical chromophores (T_g = 16 °C) in the main chain the photocurrent initially increases with increasing E_0 but substantially slows down at $E_0 > 40$ V μm^{-1}.[90] In this E_0 range the two-beam coupling gain coefficient and the diffraction efficiency reach saturation and become equal to $\Gamma = 25$ cm^{-1} and $\eta = 0.5\%$, respectively. This was explained by peculiar features of reorientation of the $Ru(bipy)_3^{2+}(PF_6^-)_2$ dipole in the E_t field. As E_t increases, the PF_6^- anion changes its position relative to the cation and the direction of the dipole moment of this ion group changes. The dipole induces an internal local electric field. The stronger the E_0 field, the better the dipole alignment along the E_t direction and the stronger the internal local field. The local field is directed oppositely to the E_t field; therefore, the growth of the effective field E_t' responsible for the creation of a grating is restricted.[90]

V. The gain coefficient and diffraction efficiency in photorefractive polymeric systems

The most important characteristics of recently developed photorefractive polymeric systems are listed in Table 3. The two-beam coupling gain coefficients of these composites were measured both at equal beam intensities [$\beta = I_1(0)/I_2(0) = 1$, see formula (15)] and at $\beta > 1$ to avoid 'depletion' of the pump beam.

Taking the PVCz/TNF-composites containing the chromophores *N*,*N*-diethyl-*p*-nitroaniline or 4-(hexyloxy)nitrobenzene as examples, it was shown[91] that the two-beam coupling gain coefficient in the PR layers is independent of β and close to 10 or 3 cm^{-1}, respectively, in the range of β variation from 0.8 to 81. A very weak dependence of Γ on β (Γ increases from 5 to 10 cm^{-1} as β increases from 1 to ~500) was found for inorganic crystals.[5]

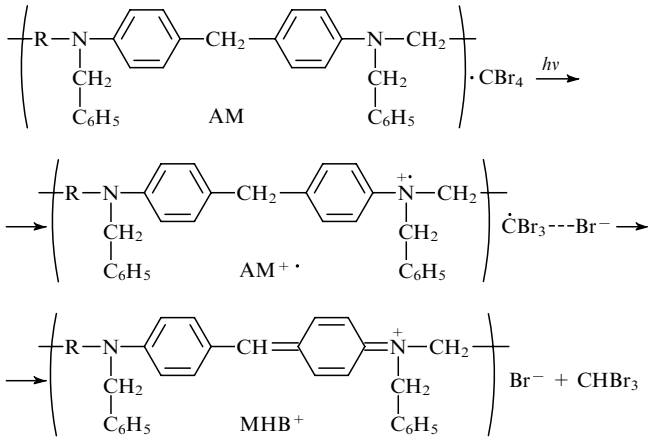
Currently, PR-materials with low glass transition temperatures (*i.e.*, close to room temperature or below it) have been the subject of intensive research and development. The T_g values were lowered by introducing plasticisers. In such composites the grating is created due to the orientation polarisation of chromophores in the E_t field.[10, 12, 31 – 33, 52, 56, 62, 73, 74, 76, 87, 92 – 105] The composites listed in Table 3 (except for the composite No. 14 with triphenylamino transport groups incorporated into the main chain[100]) include polymers such as PVCz, polysiloxanes or polyacrylates with the carbazolyl transport groups in the side chains. In these systems phototransfer of an electron by reaction (23) is followed by hole hopping from bright fringes to the dark regions in the E_0 field (see Fig. 2*b*). Fullerene C_{60} and a charge transfer complex between the donor carbazolyl group of the polymer and the acceptors, TNF or its derivative TNFDM, are used as sensitisers. The composites sensitised with C_{60} fullerene are characterised by high quantum yields of charge carriers, since the recombination stage of reaction (23) is impeded due to the long distance between the charges owing to electron delocalisation over the bulky C_{60} molecule.[103] A feature of the composite No. 12 is the possibility of simultaneously writing the PR-grating and a local photochemical grating.[99] The creation of the latter is due to energy transfer from the triply excited fullerene to the nonlinear optical chromophore, which occurs simultaneously with the process (23). The excited chromophore enters into the [2+2]-cycloaddition reaction with the non-excited chromophore, thus creating a photochemical phase grating which is not shifted in phase relative to the bright fringes. Simultaneous creation of two gratings was also found in the composite comprised of neutral PMMA, DEH and a nonlinear optical chromophore (DO-3 dye).[104] Laser-induced photoexcitation of the dye at 514 nm is followed by phototransfer of an electron, its trapping by the acceptor group of the dye ($NO_2^{-\bullet}$), generation of a mobile hole ($DEH^{+\bullet}$)

$$(DO\text{-}3)^* + DEH \longrightarrow (DO\text{-}3)^{-\bullet} + DEH^{+\bullet},$$

thus causing the appearance of photocurrent and the refractive index modulation.

The γ_0 value at an external field strength of 8 V μm^{-1} is 1.065. The PR effect is masked by the effect of a reversible increase in the intensities of both beams by 12%. The latter effect is due to *trans*–*cis*-photoisomerisation of the DO-3, which is accompanied by a nearly seven-fold decrease in the absorption coefficient.[105]

A single-component photorefractive polymer layer was obtained by photochemical modification (PM) of poly(hydroxyaminoether), PHAE (see Table 3, compound No. 22).[106 – 109] The layers comprised of PHAE with donor amino groups (AM) incorporated into the main chain and the CBr_4 acceptor groups were photochemically modified. The amino group and CBr_4 form photosensitive charge-transfer complexes characterised by optical absorption in the region 330 – 500 nm. Exposure to light in this spectral region results in the formation of chromophores of the Michler hydrol (MHB^+) type due to phototransfer of charge.



Here R is the hydroxyether fragment responsible for the adhesive and other properties.

After removal of CBr_4 from the layer by heating, the exposed areas of the polymer layer consisted of the PHAE with the modified main chain containing conjugated MHB^+Br^- fragments that absorb light in the region 560 – 700 nm and are responsible for the photoelectric sensitivity of PM PHAE[110] and for the second-order nonlinear optical properties.[111] When writing a PR-grating using two beams of an Ar–Kr laser (λ = 647 nm), photoexcitation of MHB^+ Br^- in the region of bright fringes is followed by phototransfer

$$MHB^+Br^- \longrightarrow (MHB^+Br^-)^* \longrightarrow MHB^{\bullet}Br^- + AM^{+\bullet},$$

which is accompanied by trapping of electrons ($MHB^{\bullet}Br^-$) and the formation of mobile holes

$$AM + AM^{+\bullet} \longrightarrow AM^{+\bullet} + AM,$$

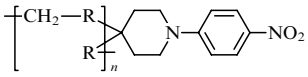
which migrate in the E_0 field and are trapped in the dark regions, thus forming the space-charge field E_{sc}.

Table 3. Most important characteristics of polymeric photorefractive composites comprising a polymer, a sensitiser, a plasticiser and a chromophore.

No.	Polymer	Sensitiser	Plasticiser	Chromophore	β	T_g /°C	d /μm	λ /nm	α /cm^{-1}	E_0 /V μm^{-1}	Γ /cm^{-1}	$10^3\,\Delta n$	τ_e /s	η (%)	$(\Gamma-\alpha)$ /cm^{-1}	Ref.
1	PVCz	TNF	ECz	**11**	1, 3	21	105	675	13	90	220	5.5	–	86	207	12, 31
2	PVCz	C_{60}	BBP	PDCST	1	28	75	676	12	120	200	–	0.05		188	32, 94, 95
3	PVCz	TNF		BDMNPAB	1	20	100	633	~13	92.4	195	4.3	~3	15	182	52
4	PSX-Cz	TNF		**11**	1	25	40	670	–	80	220	10	5	60	~220	56
5	PVCz	TNF	ECz	**11**	1	20	105	675	–	60	–	1.2	~3	86	–	96
6	PVCz	TNFDM	ECz	DHADC-MPN	1	20	105	830	–	59	–	1.5	~3	74	–	96
7	PVCz	TNF	ECz	**11** + **8**	100	21	105	790	15	60	140	2	2	85	125	62
8	PVCz	C_{60}	BBP	DCST	37	28	135	676	9	50	60	–	0.057	–	51	93
9	PSX-Cz [a]				1	43	100	676	5.4	40	22	–	2.8	–	16.6	97
10	PVCz	C_{60}	TCP	APSS	1	20	180–195	488, 514	48, 33	65	63, 110	–	~3	–	15, 37	98
								633	8		51	–	~3	–	43	98
11	PVCz	C_{60}	BBP	AODCST	1	20	100	647	9	100	235	1.3	0.05	–	226	51, 53
		C_{60}	BBP	AODCST	2000	20	260	647	~26	77	166	–	0.033	–	140	92
12	PVCz	C_{60}	BBP	Lemke-e	1	26	75	675	–	82	156	1.3	1	50	~156	99
13	PVCz	C_{60}	TCP	**7**	1	20	100	633	3.3	80	107	0.6	0.35	15.5	104	100
14	TDPANA-FA	C_{60}	TCP	–	1	20	100	633	4.7	80	36.1	–	0.004	–	31.4	100
15	PVCz	TNFDM	ECz	MHADC-MPN	1	21	125	780	13	60	167	1.6	0.72	86	154	73
16	PVCz	TNFDM	ECz	**14**	1	21	102	780	–	60	70	0.9	–	25	~70	33, 74
		TNFDM	ECz	**15**	1	21	102	780	–	60	88	1.4	–	40	~88	33, 74
		TNFDM	ECz	**16**	1	21	102	780	–	60	167	3.1	–	85	~167	33, 74
17	PSX-Cz	TNFDM		**4**	1	25	105	633	42	33.3	72	–	~600	–	30	38
18	PSX-Cz	TNF		**12**	1	30	100	676	33	80	130	–	~0.5	–	97	87
		TNF		**13**	1	28	150		20		80	–		–	60	87
19	PSX-Cz	TNF		DB-IP-DC	1	27	100	633	–	30	–	3	~10	92	–	101
20	CPA	TNF	ECz		1	20	100	633	–	92.4	93	0.5	–	12	~93	102
21	PMMA-Cz	TNFDM	LC (20%	**17**	1	15	125	780	–	48	70	–	–	–	~70	76
			by mass)	**18**, **19**	1	10	125	780	–	48	35	–	–	–	~35	76
22	PM PHAE	MHB^+	MHB^+		1	74	19.4		66	26	189	–	19	–	117	106–109
23	API	J-aggregates	Dye 1		1	230	5	514	362	16	480	5	3	2.3	118	29, 30
		J-aggregates	Dye 1		1	230	5	647	37	123	398	–	2.5	–	361	80
		J-aggregates	Dye 2		1	230	4	633	75	50	218	4	0.02	3	143	80

[a] With chromophore side groups.

Note. BBP is butyl benzyl phthalate; PDCST is 4-piperidinodicyanostyrene-malononitrile; BDMNPAB is 1-n-butoxy-2,5-dimethyl-4-(4′-nitrophenylazo)benzene; DHADC-MPN is 2-*N*,*N*-dihexylamino-7-dicyanomethylidenyl-3,4,5,6,10-pentahydronaphthalene; DCST is dicyanostyrene; APSS is 4-[*N*-(2-hydroxyethyl)-*N*-methylamino]-4′-(6-hydroxyhexylsulfonyl]stilbene; TCP is tricresyl phosphate; AODCST is aminodioctyldicyanostyrene; Lemke-e is (3-{2-[4-(*N*,*N*-diethylamino)phenyl]vinyl}-5,5-dimethylcyclohex-2-enylidene)malonodinitrile; MHADC-MPN is *N*,*N*-methylhexylamino-7-dicyanomethylidenyl-3,4,5,6,10-pentahydronaphthalene; DB-IP-DC is {3-[(*E*)-2-dibutylaminovinyl]-5,5-dimethylcyclohex-2-enylidene}malononitrile; CPA is a copolymer of carbazolyl acrylate and 1-(acryloxyethyloxy)-2,5-dimethyl-4-(nitrophenylazo)benzene;

TDPANA-FA is  [R = –(C$_6$H$_4$)–N(C$_6$H$_4$–Me)–C$_6$H$_4$–].

The PM PHAE layers generate the second harmonic at 532 nm under the action of pulses of a Nd–YAG laser ($\lambda = 1064$ nm).[111] This is due to the fact that in Ch^+X^- compounds the outer anion X^- causes a displacement of the electron density in the cationic fragment.[43] The dipole moment thus induced interacts with the E_0 field. This interaction is responsible for the apperance of a predominant orientation of the dipole moments of the MHB^+ cations in the bulk of the polymer layer, and, hence, for the volume susceptibility $\chi^{(2)}$. The second- and third-order volume susceptibilities provide the refractive index modulation

$$\Delta n_1 = \Delta n_{PEO} + \Delta n_{KEO} = \frac{2\pi E_{sc}\left(\chi^{(2)} + \chi^{(3)} E_t\right)}{n}.$$

The MHB^+ cation can exhibit orientational polarisability despite the fact that this nonlinear optical chromophore is incorporated into the polymer chain of PM PHAE and its diffusive motion is restricted. The polarisability is due to the interaction between the cation and the mobile Br^- anion, which is displaced relative to the cation during the formation of the E_t field and changes the direction of the induced dipole moment of the MHB^+ cation, thus contributing of Δn_{OB} to the refractive index modulation.

A peculiarity of PM PHAE is that the transport centres and the photogeneration and nonlinear optical fragments formed upon exposure are embedded into the main chain. This substantially decreases the probability of the formation of dimers, which are deep hole traps. Besides, as mentioned above, compensation of dipole moments in the case of dimerisation of low-molecular-mass chromophores reduces the orientational polarisability.[62]

Table 3 lists the most important characteristics of a photorefractive polymeric material (API containing nanocrystalline J-aggregates of carbocyanine dyes) with a high glass transition temperature ($T_g = 230$ °C). J-Aggregates form a centrosymmetric structure in the polymer matrix. As mentioned above, this structure is characterised by a very high third-order susceptibility,[66] so the refractive index modulation is governed by the contribution of the Kerr electro-optic effect, Δn_{KEO} [see Eqn (7)]. Therefore, in contrast to most polymer composites listed in Table 3, in this case there is no need for pre-poling of J-aggregates in the electric field or use of viscous low-T_g polymers. As can be seen in Table 3, the PR-polymeric material with J-aggregates has a large two-beam coupling gain coefficient, the net internal gain having a record value of 361 cm^{-1}.

VI. Practical applications of polymeric photorefractive materials

Organic (in particular, polymeric) materials have long been thought as inefficient, unstable and insufficiently pure for electronic and photonic applications. Because of this the emphasis was placed on inorganic crystalline and amorphous semiconductors and dielectrics. However, considerable advances in the synthesis of and research on new organic compounds achieved during the last two decades have introduced radical changes in the situation. Suffice it to say that currently nearly 90% of photoreceptors for copiers, laser printers and digital presses are made of organic polymeric materials. What is more, novel polymers, organic compounds and materials based on them possessing photoelectric and optical properties are considered as rather promising for use in electroluminescent devices, solar energy converters, *etc*.

Such characteristics of photorefractive polymeric materials as high photoelectric sensitivity, beam coupling ratio, refractive index modulation, diffraction efficiency and short (millisecond range) hologram writing times, as well as the possibility of repeated real-time hologram writing/erasure cycles make these materials promising for photonic applications. In particular, dynamical holograms can be written with a diffraction efficiency of nearly 100% and erased by illuminating the PR-layer in the absorption band of a photogenerator. Some other applications include, *e.g.*, a unique image amplification effect, a laser-based method for detection of ultrasonic oscillations of various media [93] and a method for storage of digital information by one- and two-photon excitation of a photorefractive polymeric material.[112] It is of interest to consider the prospects for use of these materials in everyday life, which go beyond the scope of the photonics area, in more detail.

Protection of documents and goods from forgery and counterfeit is a topical problem. Current holographic techniques are no longer a solution to this problem, since holograms can be readily copied. Peyghambarian *et al.*[113] proposed a photorefractive method for security verification of objects of various nature, which is based on the ability of photorefractive polymeric materials to write dynamical holograms. A transparent phase mask of size 5×5 mm and thickness 1–2 μm is placed on an object to be verified. The mask is an array of a rather large number of pixels, the pixel size being of the order of several tens of micrometres. Such pixels are photolithographically or in another manner formed in an initial mask material in a specified order or randomly and differ from the latter in refractive index value. Using a simple optical laser correlator, the mask with a secret code is compared with the reference mask encoded exactly in the same way as the test mask. The main element of such a device is the photorefractive polymer layer (for the layer composition, see Table 3, No. 1). First, a photorefractive hologram of the test phase mask is written on the polymer by the interference of the pump beam and the signal beam and serves as a holographic filter. Then the laser beam transmitted through the reference mask passes through the polymer layer from the opposite side. This beam undergoes diffraction towards the pump beam. If the images of the reference mask and the test mask in the photorefractive polymer layer match each other, the intensity of the diffracted beam increases dramatically. The advantages of this system are low cost, nearly full protection from copying information recorded on the mask, real-time operation (response time is about 1 s), confident verification (even if 90% of information recorded on the mask is erased) and the possibility of using a small-size semiconductor laser diode for writing dynamic holograms.

Energy transfer between interfering beams in photorefractive polymer layers is used for image amplification in video-rate optical processing applications.[92] Using a conventional optical scheme with the pump and the signal beams interfering in a photorefractive polymer layer (beam intensity ratio $\beta = 2000$ at a signal beam intensity of 0.5 mW cm^{-2}), a net increase in image intensity by a factor of 37 was observed within a video frame at a $E_0 = 77$ V μm^{-1} field applied to the layer. The frame exposure time is determined by the time taken to reach the maximum net intensity gain during creation of a phase hologram in the PR layer (the layer composition is listed in Table 3, No. 11) and is 33 ms, which nearly coincides with the frame illumination time when watching a movie. As the polarity of the external field applied to the photorefractive polymer layer changes, energy is transferred from the signal beam to the pump beam. As a consequence, only moving objects can be visualised using the image-bearing laser beam. Indeed, by imaging static objects a hologram is created in the photorefractive layer and the signal beam energy is transferred to the pump beam, thus diminishing the image. If objects move faster than the photorefractive response time, the hologram has no time to be created, so no energy transfer from the signal beam occurs and the moving object can be clearly seen on a screen. Clearly, by varying the hologram writing speed in the PR layer it is possible to change the speed threshold necessary for visualisation of moving objects.

A photorefractive method of medical diagnosis has been proposed.[96] It is known that biological tissues strongly scatter radiation over the whole optical region and at the same time are transparent in the near-IR region (700 to 900 nm). Hence, tissue diagnosis requires separation of the scattered radiation from the

unscattered radiation carrying useful information about absorption centres in the medium. In addition, the material for writing dynamic holograms must be near-IR sensitive. This problem can be solved using a photorefractive polymeric material (for the composition, see Table 3, No. 6). The technique employs a time delay of the scattered radiation with respect to the unscattered radiation in the signal beam due to extension of the optical path in the scattering medium. The source of IR radiation was either a pulsed femtosecond Ti : sapphire laser (λ = 830 nm) or a semiconductor laser diode capable of generating a continuous-wave (cw) low-coherence beam. The hologram is formed only when the unscattered radiation of the signal beam overlaps with the pump beam. When using a pulsed laser, the delayed scattered radiation reaches the PR layer after the pump beam pulse; when using a cw laser, coherent portions of the unscattered beam and the pump beam interfere, while the delayed scattered radiation reaches the PR layer simultaneously with the non-coherent radiation of the signal beam. In both cases the hologram is formed only when the signal and the pump beams overlap within the coherence length of a laser source. The hologram can be reconstructed using the probe laser beam counterpropagating with the pump beam and a conventional optical scheme.

In all the systems considered above, low-T_g photorefractive polymers were used. In addition to their advantages (see above) photorefractive polymeric systems have a fundamental drawback, which precludes wide industrial applications of such materials and consists in a relatively short lifetime of stable photorefractive parameters (about six months at room temperature even when encapsulated and protected from moisture).[113] This is due to crystallisation of chromophore and phase separation within the layer. A possible solution to this problem is to work with high-T_g polymeric systems. This is of course associated with loss of alignment of the dipole chromophores in the modulated space-charge field responsible for additional increase in Δn. Therefore, search for new polymeric systems with high nonlinear susceptibilities is required. A promising avenue of investigations is the incorporation of chromophores with high third-order susceptibility into photorefractive polymeric systems. For instance, J-aggregates of carbocyanine dyes have been used.[29, 30, 80] As mentioned above, during the synthesis of a PR material J-aggregates form a centrosymmetric structure, which has a very high third-order susceptibility $\chi^{(3)}$. Hence there is no need for alignment of J-aggregates in the electric field, which is necessary if one operates with photorefractive polymers possessing linear orientational polarisability and second-order nonlinearity. The refractive index modulation, Δn, is determined by the Kerr electro-optic effect and is proportional to $E_t^2\chi^{(3)}$; hence, there is no need to use low-T_g polymers.

Besides, the electronic nature of optical nonlinearity allows one to expect a substantial shortening of the writing time of dynamical holograms, which in this case is not related to the orientational motion of bulky chromophores. It should also be noted that, depending on their structure, carbocyanine dyes absorb in the whole visible region and in the near IR region. J-Aggregates of carbocyanine dyes are nanocrystalline particles, which absorb the electromagnetic radiation at wavelengths that are 100 – 300 nm longer than the absorption wavelengths of the corresponding monomeric dye molecules. Thus, in principle the long-wavelength limit of the sensitivity of photorefractive polymeric materials can be estimated at 1550 nm. The fact that optical fibre communication operates at this wavelength significantly extends the range of practical applications of such materials. Oligomeric triacetylene and diacetylene compounds characterised by high third-order susceptibility (see above) can also be used as chromophores.

This review has been written with the financial support of the International Scientific and Technological Centre (Grant 2207) and the Russian Foundation for Basic Research (Project No. 02-03-33052).

References

1. A Ashkin, G D Boyd, J M Dziedzic, R G Smith, A A Ballman, J J Levinstein, K Nassau *Appl. Phys. Lett.* **9** 72 (1966)
2. K Sutter, J Hulliger, P Günter *Solid State Commun.* **74** 867 (1990)
3. S Ducharme, J C Scott, R J Twieg, W E Moerner *Phys. Rev. Lett.* **66** 1846 (1991)
4. W E Moerner, S M Silence *Chem. Rev.* **94** 127 (1994)
5. N V Kukhtarev, V B Markov, S G Odulov, M S Soskin, V L Vinetskii *Ferroelectrics* **22** 949 (1979)
6. D M Burland, R D Miller, C A Walsh *Chem. Rev.* **94** 31 (1994)
7. D R Kanis, M A Ratner, T J Marks *Chem. Rev.* **94** 195 (1994)
8. A V Vannikov, A D Grishina, R V Rikhval'skii, A T Ponomarenko *Usp. Khim.* **67** 507 (1998) [*Russ. Chem. Rev.* **67** 451 (1998)]
9. A Dhinojwala, G K Wong, J M Torkelson *J. Opt. Soc. Am. B* **11** 1549 (1994)
10. W E Moerner, S M Silence, F Hache, G C Bjorklund *J. Opt. Soc. Am. B* **11** 320 (1994)
11. I C Khoo, H Li, Y Liang *Opt. Lett.* **19** 1723 (1994)
12. B Kippelen, K Meerholz, N Peyghambarian, in *Nonlinear Optics of Organic Molecules and Polymers* (Eds H S Nalwa, S Miyata) (Boca Raton, FL: CRC Press, 1997) p. 465
13. H Ono, I Saito, N Kawatsuki *Appl. Phys. B* **66** 527 (1998)
14. J L Oudar, D S Chemla *J. Chem. Phys.* **66** 2664 (1977)
15. F Würthner, R Wortmann, K Meerholz *Chemphyschem.* **3** 17 (2002)
16. R Wortmann, C Poga, R J Twieg, C Geletneky, C R Moylan, P M Lundquist, R G DeVoe, P M Cotts, H Horn, J E Rice, D M Burland *J. Chem. Phys.* **105** 10637 (1996)
17. E V Rudenko, A V Sukhov *Pis'ma ZhETF* **59** 133 (1994) [a]
18. E V Rudenko, A V Sukhov *Zh. Eksp. Teor. Fiz.* **105** 1624 (1994) [b]
19. I C Khoo *IEEE J. Quantum Electron.* **32** 525 (1996)
20. H Kogelnik *Bell Syst. Tech. J.* **48** 2909 (1969)
21. D L Staebler, J J Amodei *J. Appl. Phys.* **43** 1042 (1972)
22. J P Huignard, A Marrakchi *Opt. Commun.* **38** 249 (1981)
23. V L Vinetskii, N V Kukhtarev *Dinamicheskaya Golografiya* (Dynamic Holography) (Kiev: Naukova Dumka, 1983)
24. M P Petrov, S I Stepanov A V Khomenko *Photorefractive Crystals in Coherent Optical Systems* (Berlin: Springer, 1991)
25. P Yeh *Introduction to Photorefractive Nonlinear Optics* (New York: Wiley, 1993)
26. D D Nolte, in *Photorefractive Effects and Materials* (Ed. D D Nolte) (London: Kluwer Academic, 1995) p. 1
27. K Buse *Appl. Phys. B* **64** 273 (1997)
28. Y Guo, L Liu, Y Liu, C Zhou *Opt. Commun.* **180** 153 (2000)
29. A V Vannikov, A D Grishina, B I Shapiro, L Ya Pereshivko, T V Krivenko, V V Savelyev, V I Berendyaev, R W Rychwalski *Nonlinear Opt.* **29** 7 (2002)
30. A V Vannikov, A D Grishina, B I Shapiro, L Ya Pereshivko, T V Krivenko, V V Savel'ev, V I Berendyaev, R V Rikhval'skii *Khim. Vys. Energ.* **36** 430 (2002) [c]
31. K Meerholz, B L Volodin, Sandalphon, B Kippelen, N Peyghambarian *Nature (London)* **371** 497 (1994)
32. A Grunnet-Jepsen, C L Thompson, R J Twieg, W E Moerner *Appl. Phys. Lett.* **70** 1515 (1997)
33. D Van Steenwinckel, E Hendrickx, K Van Den Broeck, C Samyn, A Persoons *Nonlinear Opt.* **25** 219 (2000)
34. S M Silence, M C J M Donckers, C A Walsh, D M Burland, W E Moerner *Appl. Phys. Lett.* **64** 712 (1994)
35. B Kippelen, F Meyer, N Peyghambarian, S R Marder *J. Am. Chem. Soc.* **119** 4559 (1997)
36. A Fort, J Muller, O Cregut, J P Vola, M Barzoukas *Opt. Mater.* **9** 271 (1998)
37. A Fort, J Muller, L Mager *Chem. Phys.* **243** 115 (1999)
38. A Fort, L Mager, J Muller, C Combellas, G Mathey, A Thiebault *Opt. Mater.* **12** 339 (1999)
39. C R Moylan, R Wortmann, R J Twieg, I-H McComb *J. Opt. Soc. Am. B* **15** 929 (1998)
40. R Wortmann, C Glania, P Krämer, K Lukaszuk, R Matschiner, R J Twieg, F You *Chem. Phys.* **245** 107 (1999)
41. M Barzoukas, M Blanchard-Desce *J. Chem. Phys.* **112** 2036 (2000)

42. R S Mulliken, W B Person *Molecular Complexes* (London: Wiley, 1969)
43. C B Gorman, S R Marder *Proc. Natl. Acad. Sci. USA* **90** 11 297 (1993)
44. S R Marder, J W Perry, G Bourhill, C B Gorman, B G Tiemann, K Mansour *Science* **261** 186 (1993)
45. G Bourhill, J-L Brédas, L-T Cheng, S R Marder, F Meyers, J W Perry, B G Tiemann *J. Am. Chem. Soc.* **116** 2619 (1994)
46. F Meyers, S R Marder, B M Pierce, J-L Brédas *J. Am. Chem. Soc.* **116** 10 703 (1994)
47. A D Grishina, L Ya Pereshivko, T V Krivenko, V V Savel'ev, J Vernel, R W Rychwalski, A V Vannikov *Polymer* **42** 4837 (2001)
48. M J Kubat, J Vernel, R W Rychwalski, J Kubat *Polym. Eng. Sci.* **38** 1261 (1998)
49. J-L Brédas, C Adant, P Tackx, A Persoons, B M Pierce *Chem. Rev.* **94** 243 (1994)
50. A Grunnet-Jepsen, C L Thompson, R J Twieg, W E Moerner *Appl. Phys. Lett.* **70** 1515 (1997)
51. D Wright, M A Diaz-Garcia, J D Casperson, M De Clue, W E Moerner, R Twieg *Appl. Phys. Lett.* **73** 1490 (1997)
52. F Wang, Z Chen, Q Gong, Y Chen, H Chen *Appl. Phys. B* **67** 207 (1998)
53. M A Diaz-Garcia, D Wright, J D Casperson, B Smith, E Glazer, W E Moerner, L I Sukhomlinova, R J Twieg *Nonlinear Opt.* **25** 189 (2000)
54. F Würthner, S Yao, J Schilling, R Wortmann, M Redi-Abshiro, E Mecher, F Gallego-Gomez, K Meerholz *J. Am. Chem. Soc.* **123** 2810 (2001)
55. J Wolff, S Schloter, U Hofmann, D Haarer, S J Zilker *J. Opt. Soc. Am. B* **16** 1080 (1999)
56. S Schloter, U Hofmann, P Struhriegl, H-M Schmidt, D Haarer *J. Opt. Soc. Am. B* **15** 2473 (1998)
57. N Kim, H Chun, W S Jahng, S D Song, D-H Shin, M Joo *Nonlinear Opt.* **25** 67 (2000)
58. J Sohn, S Y Park, H Moon, J Mun, C S Yoon *React. Funct. Polym.* **45** 109 (2000)
59. S Schloter, U Hofmann, K Hoechstetter, G Bäuml, D E Ewert, C-D Eisenbach *J. Opt. Soc. Am. B* **15** 2561 (1998)
60. R Bittner, C Bräuchle, K Meerholz *Appl. Opt.* **37** 2843 (1998)
61. D J Binks, K Khand, D P West *J. Opt. Soc. Am. B* **18** 308 (2001)
62. K Meerholz, Y De Nardin, R Bittner, R Wortmann, F Würthner *Appl. Phys. Lett.* **73** 4 (1998)
63. U Gubler, Ch Bossard, P Günter, M Y Balakina, J Cornil, J L Brédas, R E Martin, F Diederich *Opt. Lett.* **24** 1599 (1999)
64. M G Kusyk *Phys. Rev. Lett.* **85** 1218 (2000)
65. M G Kusyk *Opt. Lett.* **25** 1183 (2000)
66. V V Shelkovnikov, R V Markov, A I Plekhanov, A E Simanchuk, Z M Ivanova *Khim. Vys. Energ.* **36** 295 (2002) [c]
67. R Gadonas, in *J-Aggregates* (Ed. T Kobayashi) (Singapore: World Scientific, 1996) p. 181
68. K Misawa, T Kobayashi, in *J-Aggregates* (Ed. T Kobayashi) (Singapore: World Scientific, 1996) p. 41
69. J Knoester *Chem. Phys. Lett.* **203** 373 (1993)
70. M Schott, G Wegner, in *Nonlinear Optical Properties of Organic Molecules and Crystals* Vol. 2 (Eds D S Chemla, J Zyss) (New York: Academic Press, 1987) Ch. 10
71. F Kajzar, J Messier, in *Nonlinear Optical Properties of Organic Molecules and Crystals* Vol. 2 (Eds D S Chemla, J Zyss) (New York: Academic Press, 1987) Ch. 11
72. G M Carter, Y J Chen, M F Rubner, D I Sandman, M K Thakur, S K Tripathy, in *Nonlinear Optical Properties of Organic Molecules and Crystals* Vol. 2 (Eds D S Chemla, J Zyss) (New York: Academic Press, 1987) Ch. 12
73. I Ledoux, I D W Samuel, J Zuss, S N Yaliraki, F J Schattenmann, R R Schrock, R J Silbey *Chem. Phys.* **245** 1 (1999)
74. D Van Steenwinckel, E Hendrickx, A Persoons, K Van den Broeck, C Samyn *J. Chem. Phys.* **112** 11 030 (2000)
75. E Hendrickx, Y Zhang, K B Ferrio, J A Herlocker, J Anderson, N R Armstrong, E A Mash, A P Persoons, N Peyghambarian, B Kippelen *J. Mater. Chem.* **9** 2251 (1999)
76. D Van Steenwinckel, E Hendrickx, C Samyn, C Engel, A Persoons *J. Mater. Chem.* **10** 2692 (2000)
77. G G Malliararas, V V Krasnikov, H J Bolink, G Hadziioannou *Appl. Phys. Lett.* **66** 1038 (1995)
78. D P West, M D Rahn, C Im, N Bässler *Chem. Phys. Lett.* **326** 407 (2001)
79. A D Grishina, L Ya Pereshivko, T V Krivenko, B I Shapiro, A V Vannikov *Khim. Vys. Energ.* **37** 204 (2003) [c]
80. A V Vannikov, A D Grishina, B I Shapiro, L Ya Pereshivko, T V Krivenko, V V Savelyev, V I Berendyaev, R W Rychwalski *Chem. Phys.* **287** 261 (2003)
81. A R Tameev, A A Kozlov, E I Mal'tsev, D A Lypenko, V V Bobinkin, A V Vannikov *Org. Light-Emitting Mater. Devices IV, Proc. SPIE* **4105** 443 (2001)
82. L P Kazakova, E L Aleksandrova, A V Chernyshev *Fiz. Tekh. Poluprovodn.* **35** 695 (2001)
83. A Mozumder *J. Chem. Phys.* **60** 4300 (1974)
84. P J Melz *J. Chem. Phys.* **57** 1694 (1972)
85. P M Borsenberger, D S Weiss *Organic Photoreceptor for Xerography* (New York: Marcel Dekker, 1998)
86. M Pope, C E Swenberg *Electronic Processes in Organic Crystals and Polymers* (Oxford, New York: Oxford University Press, 1999)
87. S Wu, F Zeng, F Li, J Li *React. Funct. Polym.* **46** 225 (2001)
88. A Goonesekera, S Ducharme *J. Appl. Phys.* **85** 6506 (1999)
89. E Mecher, R Bittner, C Bräuchle, K Meerholz *Synth. Met.* **102** 993 (1999)
90. L Wang, Q Wang, L Yu *Appl. Phys. Lett.* **71** 2546 (1998)
91. G G Malliaras, Ph.D. Thesis, Groningen University, Groningen, Nederland, 1995
92. A Goonesekera, D Wright, W E Moerner *Appl. Phys. Lett.* **76** 3358 (2000)
93. M B Klein, G D Bacher, A Grunnet-Jepsen, D Wright, W E Moerner *Opt. Commun.* **162** 79 (1999)
94. A Grunnet-Jepsen, C L Tompson, R I Twieg, W E Moerner *J. Opt. Soc. Am. B* **15** 901 (1998)
95. A Grunnet-Jepsen, C L Tompson, W E Moerner *J. Opt. Soc. Am. B* **15** 905 (1998)
96. B Kippelen, S R Marder, E Hendrickx, J L Maldonado, G Guillemen, B L Volodin, D D Steele, Y Enami, Sandalphon, Y J Yao, J F Wang, H Röckel, L Erskine, N Peyghambarian *Science* **279** 54 (1998)
97. M S Bratcher, M S DeClue, A Grunnet-Jepsen, D Wright, B R Smith, W E Moerner, S Siegel *J. Am. Chem. Soc.* **120** 9680 (1998)
98. K-S Kim, Y Cui, B Swedek, N Cheng, P N Prasad *Nonlinear Opt.* **20** 331 (1999)
99. S J Struts, L M Hayden *Appl. Phys. Lett.* **74** 2749 (1999)
100. S-H Park, K Ogino, H Sato *Synth. Met.* **113** 135 (2000)
101. W-J Joo, N-J Kim, H Chun, I K Moon, N Kim *Polymer* **42** 9863 (2001)
102. Y Chen, Y He, F Wang, H Chen, Q Gong *Polymer* **42** 1101 (2001)
103. D V Konarev, R I Lyubovskaya *Usp. Khim.* **68** 23 (1999) [*Russ. Chem. Rev.* **68** 19 (1999)]
104. A V Vannikov, A D Grishina, L Ya Pereshivko, T V Krivenko, V V Savel'ev, L I Kostenko, R V Rikhval'skii *Vysokomol. Soedin., Ser. A* **43** 977 (2001) [d]
105. S Yu Grenkin, B V Bol'shakov *J. Polym. Sci., Part B: Polym. Phys.* **37** 1753 (1999)
106. A V Vannikov, A D Grishina, L Ya Pereshivko, T V Krivenko, R W Rychwalski *Nonlinear Opt.* **28** 107 (2001)
107. A V Vannikov, A D Grishina, L Ya Pereshivko, T V Krivenko, V V Savelyev, L I Kostenko, R W Rychwalski *Opt. Memory Neural Networks* **10** 147 (2001)
108. A V Vannikov, A D Grishina, L Ya Pereshivko, T V Krivenko, V V Savel'ev, L I Kostenko, R V Rikhval'skii *Khim. Vys. Energ.* **36** 44 (2002) [c]
109. A V Vannikov, A D Grishina, L Ya Pereshivko, T V Krivenko, V V Savelyev, L I Kostenko, R W Rychwalski *J. Photochem. Photobiol., A* **150** 187 (2002)
110. A V Vannikov *Zh. Nauchn. Prikl. Fotogr.* **40** (2) 75 (1995) [e]
111. A D Grishina, L Ya Pereshivko, T V Krivenko, V V Savel'ev, L I Kostenko, A V Anikeev, A V Vannikov *Khim. Vys. Energ.* **33** 117 (1999) [c]

112. D Day, M Gu, A Smallridge *Opt. Lett.* **24** 948 (1999)
113. B L Volodin, B Kippelen, K Meereholz, B Javidi, N Peyghambarian *Nature (London)* **383** 58 (1996)

[a] — *J. Exp. Theor. Phys. Lett. (Engl. Transl.)*
[b] — *J. Exp. Theor. Phys. (Engl. Transl.)*
[c] — *High Energy Chem. (Engl. Transl.)*
[d] — *Polym. Sci. (Engl. Transl.)*
[e] — *Sci. Appl. Photogr. (Engl. Transl.)*